

Detecting the oldest geodynamo and attendant shielding from the solar wind: Implications for habitability

John A. Tarduno^{a,b,*}, Eric G. Blackman^b, Eric E. Mamajek^b

^a*Department of Earth and Environmental Sciences, University of Rochester, Rochester, New York, 14627, USA*

^b*Department of Physics and Astronomy, University of Rochester, Rochester, New York, 14627, USA*

Abstract

The onset and nature of the earliest geomagnetic field is important for understanding the evolution of the core, atmosphere and life on Earth. A record of the early geodynamo is preserved in ancient silicate crystals containing minute magnetic inclusions. These data indicate the presence of a geodynamo during the Paleoproterozoic, between 3.4 and 3.45 billion years ago. While the magnetic field sheltered Earth's atmosphere from erosion at this time, standoff of the solar wind was greatly reduced, and similar to that during modern extreme solar storms. These conditions suggest that intense radiation from the young Sun may have modified the atmosphere of the young Earth by promoting loss of volatiles, including water. Such effects would have been more pronounced if the field were absent or very weak prior to 3.45 billion years ago, as suggested by some models of lower mantle evolution. The frontier is thus trying to obtain geomagnetic field records that are $\gg 3.45$ billion-years-old, as well as constraining solar wind pressure for these times. In this review we suggest pathways for constraining these parameters and the attendant history of Earth's deep interior, hydrosphere and atmosphere. In particular, we discuss new estimates for solar wind pressure for the first 700 million years of Earth history, the compet-

*Corresponding author: Tel. 585 275 5713 fax 585 244 5689 E-mail address: john.tarduno@rochester.edu

ing effects of magnetic shielding versus solar ion collection, and bounds on the detection level of a geodynamo imposed by the presence of external fields. We also discuss the prospects for constraining Hadean-Paleoarchean magnetic field strength using paleointensity analyses of zircons.

Keywords: Geodynamo, Early Earth, Solar Wind, Atmospheric Loss, Habitability

1. Introduction

The onset and nature of the geomagnetic field is important for understanding the evolution of the core, atmosphere and life on Earth. For the earliest Earth, the dynamo was powered thermally, so dynamo startup provides information on core heat flow and lower mantle conditions. A common posit is that the lack of magnetic shielding of cosmic radiation is inconsistent with the development of life, but it is clear that an atmosphere and ocean layer can provide some protection. The primary issue explored here is the survival of the hydrosphere. The magnetic field acts to prevent atmospheric erosion by the solar wind. In the case of the early Earth, the magnetic field would have had to balance the greatly enhanced solar wind pressure associated with the young rapidly-rotating Sun. The interplay between the magnetic field and radiation from the young Sun controls the loss of light elements and, ultimately, water and therefore may be a fundamental stage in the development of a habitable planet.

The interaction of the solar wind and the geomagnetic field produces Earth's magnetosphere (Figure 1), with the magnetopause (r_s) defined as the point toward the Sun (the sub-solar point) where the wind pressure is balanced by the magnetic field (Gri  meier et al., 2004):

$$r_s = \left[\frac{\mu_0 f_0^2 M_E^2}{4\pi^2 (2\mu_0 n_{sw} m_p v_{sw}^2 + B_{IMF}^2)} \right]^{1/6} \quad (1)$$

where M_E is Earth's dipole moment, n_{sw} is solar wind density, v_{sw} is solar

wind velocity, f_0 is a magnetospheric form factor (=1.16 for Earth), μ_0 is the permeability of free space, m_p is a proton mass and B_{IMF} is the interplanetary magnetic field.

Today, Earth’s magnetic field stands off the solar wind to a distance between 10 and 11 Earth radii. The occurrence of magnetic storms and their associated phenomena– including auroral lights seen at unusually low latitudes – are a vivid reminder that the solar input side of this balance is variable. In the case of a magnetic storm, a coronal mass ejection impinges on and compresses the magnetosphere, greatly reducing the magnetopause standoff distance.

Of course, Earth’s magnetic field is dynamic and it also varies on a wide range of timescales. At any given time, the geomagnetic field at a radius r , colatitude θ and longitude ϕ can be specified by the gradient of the scalar potential (Φ):

$$\Phi(r, \theta, \phi) = r_e \sum_{l=1}^{\infty} \sum_{m=0}^l \left(\frac{r_e}{r} \right)^{l+1} P_l^m(\cos\theta) [g_l^m \cos m\phi + h_l^m \sin m\phi] \quad (2)$$

where P_l^m are partially normalized Schmidt functions, r_e is the radius of Earth and the Gauss coefficients g_l^m and h_l^m describe the size of spatially varying fields. The current field is approximately 80% dipolar and when averaged over several hundred thousand years to 1 million years, the axial dipole term (g_0^1) is thought to dominate. The latter assumption– the geocentric dipole hypothesis– forms the basis of tectonic interpretations of paleomagnetic data that have been essential in our understanding of the plate tectonic history of the planet.

Paleomagnetic directions provide the opportunity for tests of the geocentric dipole hypothesis (Irving, 1964) and these have confirmed the hypothesis for times as old as ~ 2.5 billion years (Smirnov and Tarduno, 2004), notwithstanding considerable gaps in the paleomagnetic database of directions. For even deeper time, the global distribution of data does not yet permit a test, but we can proceed because the geocentric dipole assumption provides the maximum magnetic shielding (Siscoe and Sibeck, 1980).

The key magnetic parameter to determine in learning about solar-terrestrial

interactions in the deep past (eqn 1) then is magnetic field strength (M_E), but this is far more difficult to determine than paleodirections. Determining the ancient solar wind pressure is also challenging, especially for the first ~ 700 million years of Earth’s history.

In this review, we will first tackle the observational challenge of determining ancient field strength by means of examples through Paleoarchean times. We will show how these data, when combined with constraints based on solar analogs, allow us to constrain the magnetopause some 3.45 billion years ago. We provide a review of atmospheric escape mechanisms, including contrarian views that question the importance of a shield created by the geomagnetic field. Within this context, we discuss the implications of the Paleoarchean magnetopause conditions for the evolution of Earth’s water inventory. As one peers back further in time, these data mark the bifurcation point for potential trajectories for the dynamo. In one scenario, the dynamo starts soon after core formation and has been relatively strong ever since. In another, the dynamo started between 4 and ~ 3.5 billion years ago. We will next suggest ways to extend the record of the magnetopause back in time to the earliest Paleoarchean and Hadean Earth. To address the presence/absence question about the earliest field we also address the question of “recording zero” and in so-doing revisit the self-shielding potential of a planet lacking a magnetic field.

2. The Challenge of Recording Magnetic Deep Time

Stevenson (1983) suggested that field strength might approximately scale with rotation, while cautioning over the accuracy of any scaling laws of the time. Nevertheless, scaling with rotation has been suggested as a viable way of determining past field strength (Dehant et al., 2007; Lichtenegger et al., 2010). While there are many unresolved issues in dynamo theory, it is generally accepted that core convection is driven by buoyancy (e.g. Roberts and Glatzmaier, 2000), in which case intensity estimates based solely on rotation are illusory. Clearly,

observations are needed.

Obtaining paleomagnetic constraints on the oldest geodynamo, however, is difficult because of the ubiquitous metamorphism that has affected Paleoarchean and older rocks. It is sometimes assumed that the maximum metamorphic temperature can be simply related to the temperature at which a magnetization is removed from a sample in the laboratory. By this line of reasoning, if a rock had been heated to 320 °C during a metamorphic event, say for 1 million years, its magnetization isolated by heating in the laboratory to 320 °C would record the magnetic field at the time of the metamorphic event. The magnetization isolated at temperatures greater than 320 °C might record the field when the rock first cooled. In reality, many (if not most) bulk rock samples would be totally remagnetized during this metamorphic event, and/or their magnetic field strength records might be forever compromised. To understand why this is so, and how we might see through metamorphism, we must first consider the basis for measurement of past field strength (the subdiscipline of paleointensity).

2.1. Paleointensity measurement

The physical mechanism of magnetization that is best understood is that of thermoremanent magnetization (TRM), acquired when a sample’s constituent minerals cool through their Curie temperatures. To recover paleointensity from rocks carrying a TRM, the most robust method is the Thellier approach, named after seminal work of the Thelliers (Thellier and Thellier, 1959), or some of its more common variants (e.g. the Thellier-Coe approach; Coe, 1967). In these experiments, samples are exposed to a series of paired heating steps (Figure 2). For example, in the Thellier-Coe approach, a sample might first be heated to 100 °C in field free-space, during which a natural remanent magnetization (NRM) is removed. Next, the sample is reheated to the same temperature, but this time in the presence of a known applied field (this is called the “field-on” step). After cooling, the sample magnetization is measured and the thermoremanent magnetization acquired can be calculated. Because one knows the magnetiza-

tion lost, the magnetization gained and the applied field (H_{lab}), one can solve for the ancient field (H_{paleo}) recorded by the 100 °C temperature range:

$$H_{\text{paleo}} = \frac{M_{\text{NRM}}}{M_{\text{TRM}}} H_{\text{lab}} \quad (3)$$

In practice, one conducts this experiment at many steps up to the maximum Curie temperature of the magnetic minerals in a given specimen.

2.2. Chemical change

The need for the second, or “field-on” step makes paleointensity experiments far less successful than a study of magnetic directions alone. The main problem is that heating can induce changes in magnetic minerals, changing the TRM-capacity; because the measurement is done in the presence of a field, the reference needed for equation 3 (M_{TRM}) is compromised. In contrast, heatings for directional measurements are always done in field-free space, and a sample can suffer some alteration and still retain useful information.

Hence, finding samples that will not alter during laboratory experiments is one key requirement. This constraint is also closely related to the metamorphic and weathering history of a rock. In general, the formation of Fe-rich clays spells disaster for paleointensity recording because these can alter during paleointensity experiments to form new iron-oxides (e.g. Cottrell and Tarduno, 2000; Gill et al., 2002; Kars et al., 2012). Ultramafic rocks, including komatiitic lavas, might be thought of as good carriers of Archean fields, but the Fe-rich phyllosilicate serpentine $[(\text{Mg}, \text{Fe})_3\text{Si}_2\text{O}_5(\text{OH})_4]$ and magnetite are commonly formed in these rocks. The magnetite carries a magnetization dating to the alteration age (which is usually uncertain) and the magnetization is not a TRM; instead it is a crystallization or chemical remanent magnetization (CRM), and a straightforward tie to past field strength is lost (Yoshihara and Hamano, 2004; Smirnov and Tarduno, 2005).

2.3. Time, Temperature and Domain State

The principal magnetic mineral recorder of interest for Paleoproterozoic and older rocks is magnetite having a Curie temperatures of $\sim 580^\circ\text{C}$. Hematite, with a Curie temperature of 675°C is also a potential recorder, but its occurrence as a primary phase recording a TRM is rare relative to magnetite. Even if we have a pristine rock that has undergone no chemical change, magnetite within the rock can be remagnetized by the aforementioned 320°C metamorphic event even though the peak temperature is less than the Curie temperature of magnetite. To understand this phenomena, we start with the recognition that metamorphic heating will affect magnetic grains differently, according to their size and related domain state.

Large magnetic grains (greater than one micron, for example), are composed of multiple magnetic domains (called the multidomain, or MD, state). Even under low grade metamorphic conditions, we expect that new magnetizations will be acquired due to movement of domain walls. These new magnetizations will be recorded by some MD grains up to the Curie point of magnetite.

Small magnetite grains containing only a single domain (SD) have the potential to withstand low grade metamorphic conditions. The parameter of interest for these grains is the thermal relaxation time (τ), which can be expressed in terms of rock magnetic parameters as follows (Dunlop and Özdemir, 1997):

$$\frac{1}{\tau} = \frac{1}{\tau_0} \exp \left[-\frac{\mu_0 V M_s H_K}{2kT} \left(1 - \frac{|H_0|}{H_K} \right)^2 \right] \quad (4)$$

where τ_0 (10^{-9} s) is the interval between thermal excitations, μ_0 is the permeability of free space, V is grain volume, M_s is spontaneous magnetization, H_K is the microscopic coercive force, k is Boltzmann's constant, T is temperature, and H_0 is the applied field. This relationship is derived from Néel's (Néel, 1949, 1955) theory for single domain TRM; it was used by Pullaiah et al. (1975) to determine time-temperature relationships that can be in turn used to predict the acquisition of secondary magnetizations:

$$\frac{T_A \ln(\tau_A/\tau_0)}{M_s(T_A)H_K(T_A)} = \frac{T_B \ln(\tau_B/\tau_0)}{M_s(T_B)H_K(T_B)} \quad (5)$$

Where the two relaxation times (τ_A , τ_B) correspond to temperatures (T_A , T_B) respectively, and $H_K \gg H_0$. This relationship describes the tendency for the maximum metamorphic temperature to leak to a higher unblocking temperature range. Hence, for our example of a peak metamorphic temperature of 320 °C, and a nominal reheating duration of 1 million years, only SD unblocking temperatures up to ~400 °C should be affected (Dunlop and Buchan, 1977).

In summary, the challenges for paleointensity are those of finding samples that have not been chemically altered in nature, will not alter in laboratory, carry small single domain or single-domain like grains (called pseudo-single PSD), and are from low metamorphic grade geologic terrains. The magnetic properties of common Archean rock types vary on a grain (mineral) scale, so meeting these challenges is rarely possible using whole rock samples.

2.4. Single Crystal Paleointensity

One approach to address these challenges is a focus on the paleomagnetism of single crystals rather than bulk rocks, using the single silicate crystal paleointensity (SCP) approach. Silicate crystals are not of intrinsic magnetic interest, but they often host minute magnetic particles that are ideal magnetic recorders (Cottrell and Tarduno, 1999; Dunlop et al., 2005; Feinberg et al., 2005; Tarduno et al., 2006). In Mesozoic lavas, feldspars bearing magnetic inclusions have been shown to alter less in the laboratory than the whole rocks from which they were separated (Cottrell and Tarduno, 2000). The SCP approach (using feldspar from lavas) has been used to study geomagnetic field intensity versus reversal frequency for the last 160 million years (an inverse relation is supported; Tarduno et al., 2001, 2002; Tarduno and Cottrell, 2005), and during the Kiaman Superchron (Cottrell et al., 2008). The SCP method has also been applied to olivine from pallasite meteorites (Tarduno et al., 2012). The SCP approach has

allowed examination of the field of the Late, Middle and Early (Paleo) Archean as discussed below.

2.5. Prior Proterozoic-Archean Paleomagnetic Field Constraints

Most prior characterizations of the Archean field have been based on whole rocks and subsequent studies have revealed that metamorphism has most likely compromised their paleointensity record (see discussion in Usui et al., 2009). Below we highlight the salient observations about the field that are robust for the interval equal to and older than the Proterozoic-Archean boundary (Figure 3).

As noted earlier, there is a general consensus that the field was predominately dipolar at ~ 2.5 Ga (Smirnov and Tarduno, 2004; Biggin et al., 2008; Smirnov et al., 2011). The dynamo appears to be reversing, although the sparse rock record allows different interpretations of the reversal rate. Dunlop and Yu (2004) and Coe and Glatzmaier (2006) first argued that reversal rates might have been low. No long sedimentary sequences with paleomagnetic data are available to justify this interpretation for times before the Archean-Proterozoic boundary, and the thermal alteration of sediments of this age questions whether such data will ever be available. The interpretation is instead based on the sampling of lavas that are associated with large igneous provinces exposed in the Superior Craton of Canada (the ~ 2.5 Ga Matachewan Dikes; Halls, 1991) and in the Pilbara Craton of Western Australia (the ~ 2.7 - 2.8 Ga Fortesque Group; Strik et al., 2003). However, magmatic activity associated with these large igneous province could have occurred in pulses (as it has during the Phanerozoic). If so, much less time is represented by the rock record (than is expected by assuming continuous magmatism between available radiometric age data) and capturing only a few field reversals would be expected.

The oldest reversal documented to date is that associated with 3.1 to 3.2 Ga plutonic rocks exposed in the Barberton Greenstone Belt (Layer et al., 1998;

Tarduno et al., 2007). An older reversal has been reported from study of a purported 3.4 Ga tuff of the Barberton Greenstone Belt (Biggin et al., 2011), however the sampled rocks are sandstone and minor shale highly altered by local fluids (Axel Hofmann, personal communication). Moreover, the limited spatial sampling and interpretation by the authors of contamination of the data by lightning strikes suggests this reversal record could be an artifact.

Smirnov et al. (Smirnov et al., 2003) applied the SCP approach to ~ 2.45 Ga dikes formed close to the Proterozoic-Archean boundary from the Karelia Craton of Russia. Although the dikes were insufficient in number to completely average secular variation, the values are consistent with present-day field values. The SCP was also applied to 3.2 Ga plutons of the Barberton Greenstone Belt. These yielded a mean paleointensity that was interpreted as being within 50% of the current field value (Tarduno et al., 2007). However, this relatively large uncertainty was assigned to the field value to account for the possibility of cooling rate effects (in general, laboratory cooling rates are by necessity much faster than those in nature, motivating application of correction factors). Modeling and experimental data suggest that cooling rate effects are nominal for pseudosingle domain grains (Winklhofer et al., 1997; Yu, 2011; Ferk et al., 2012). Without correction, raw data from 3.2 Ga silicate crystals are essentially indistinguishable from the modern field intensities.

A few studies of whole rocks, where the principal magnetic carriers were thought to be fine magnetite exsolved in silicate crystals, are also of note. A recent restudy of the 2.78 Ga (Feinberg et al., 2010) Modipe Gabbro indicated a virtual dipole moment of 6×10^{22} A m² (Muxworthy et al., 2013). This study lacks a field test on the age of magnetization, but the pristine nature of select outcrops suggests the magnetization could be primary. Inexplicably, Muxworthy et al. (2013) do not consider the possibility of post-emplacement tectonic tilt. Given that the in situ magnetic inclination is very steep ($I = 70^\circ$ reported in Muxworthy et al. (2013); $I = 85^\circ$ in Evans and McElhinney (1966), and $I = 89^\circ$ in Feinberg et al. (2010)), it is most likely that the true paleolatitude is shallower if the Modipe Gabbro has been tilted. Denyszyn et al. (2013) convincingly

argue that the unit has been tilted, but the exact tilting amount is uncertain. Nevertheless, the value of $6 \times 10^{22} \text{ A m}^2$ is probably an underestimate of the true field strength. Study of the Stillwater Complex yielded a high paleointensity of $92 \mu\text{T}$ (Selkin et al., 2000). After correction of anisotropy, this value was reduced to $46 \mu\text{T}$, and after application of a cooling rate correction (based on SD assumptions) the value was further lowered to $32 \mu\text{T}$, resulting in a final VDM of $4 \times 10^{22} \text{ A m}^2$. For the reasons discussed above, the cooling rate correction is an overestimate if PSD grains are present, suggesting that the Stillwater VDM reported by Selkin et al. (2000) also underestimates the true field strength.

Thus, conservatively, the hypothesis that field strength was similar (i.e. within 50%) to that of the modern field cannot be rejected for the interval from the Proterozoic boundary to the mid-Archean at 3.2 Ga. Below, we discuss in more detail the constraints for field strength for the Paleoproterozoic.

3. The magnetopause 3.45 billion years ago

Arguably the least metamorphosed Paleoproterozoic rocks are found in the Barberton Greenstone belt of the Kaapvaal Craton, South Africa. Here, the peak temperatures can be as low as $<350^\circ\text{C}$ (e.g. Tice et al., 2004). Similar rocks are found in the closely associated Nondweni Greenstone Belt also of the Kaapvaal Craton, located about 300 km south of the Barberton Greenstone Belt (Hofmann and Wilson, 2007). In both belts, dacites are found which meet the recording challenges discussed above. In a sense, they are goldilocks recorders. They have a relatively low Fe content— enough to record the ancient field, but not so much that massive amounts of secondary magnetic minerals have formed during metamorphism.

3.1. Conglomerate Test

One of the most powerful tests to determine whether a rock can retain a primary record of the magnetic field is the conglomerate test (Graham, 1949) (Figure 4). If the magnetization directions from individual clasts forming a conglomerate are the same, that direction must postdate deposition. If the magnetizations differ, the clasts may retain a record of the geomagnetic field prior to deposition, and possibly dating to the formation of the rock from which a given conglomerate clast was derived. There is an important, and sometimes overlooked, limitation with the application of this test. Because different rock types will respond differently to a given set of metamorphic conditions, the conglomerate test only applies to the lithology sampled in the conglomerate test.

In the Barberton Greenstone Belt, a ~ 3416 Ma conglomerate is found, dominated by dacite clasts. Usui et al. (2009) found that the dacite clasts contained two distinct components of magnetization. At low to intermediate unblocking temperatures, the magnetization from many clasts defined a common direction that was indistinguishable from the magnetic field during the ~ 180 million-year-old Karoo magmatic event that affected most of the Kaapvaal Craton. At high unblocking temperatures ($\gtrsim 525$ - 550 °C), another distinct component was defined; the direction of this component differed between clasts. A formal test (Watson, 1956) showed that these directions indicated that the hypothesis that these directions were drawn from a random population (as expected for a conglomerate recording a primary direction) could not be rejected at the 95% confidence interval.

The parent body of the dacite clasts is exposed in the Barberton Greenstone Belt; bulk samples show a similar component structure as that seen in the clasts, but the high unblocking temperature magnetization, while grouped (as would be expected in the parent rock) showed a scatter that was unusually high as compared to that typically seen in younger igneous rocks. It must be remembered, however, that these are from bulk samples, which typically contain a wide range of magnetic grain sizes. The largest multidomain grains, which

are seen in thin section (Usui et al., 2009), are expected to carry overprints and are likely contaminating the high unblocking temperature direction. There is also a more exotic explanation. In the absence of a geodynamo, the high scatter could reflect a variable field produced by solar interaction with the Paleoarchean atmosphere. For example, the solar wind interaction with the thick atmosphere of Venus (a planet without an internally generated magnetic field) produces an external magnetic field which is more variable and more than an order of magnitude weaker than the surface field of Earth (Zhang et al., 2007) (see also *section 7*). Hence, paleointensity becomes the key variable in evaluating these data further.

3.2. Field Intensity Values at 3.4 to 3.45 Ga

To obtain a field intensity at 3.45 Ga, Tarduno et al. (2010) sampled the source of the Barberton Greenstone Belt dacite clasts; these were supplemented with a study of 3.4 Ga dacites from the Nondweni Greenstone Belt. In both belts, dacites contain quartz phenocrysts, 0.5 to 2 mm in size, which were the target of investigation. The ideal nature of the magnetic inclusions within the phenocrysts was confirmed by rock magnetic tests (e.g. magnetic hysteresis), and Thellier-Coe paleointensity data were collected using CO₂ laser heating methods (Tarduno et al., 2007) and high resolution SQUID magnetometers (including an instrument with a 6.3 mm access bore specialized for the SCP approach).

The thermal demagnetization data show the removal of a low unblocking temperature component with heating to ~ 450 °C (Figure 2). The unblocking characteristics of this component agree with single domain theory suggesting that given a peak metamorphic temperature of 350 °C, an overprint should leak to slightly higher temperatures. At higher unblocking temperatures a component is isolated that trends to the origin of orthogonal vector plots of the magnetization. Over this higher unblocking temperature range, paleointensities of 28.0 ± 4.3 μ T and 18.2 ± 1.8 μ T were obtained for the Barberton and

Nondweni dacites, respectively.

Because paleointensity is derived from a comparison of field-on versus field-off steps, it does not require one to have oriented specimens. However, oriented samples are required to obtain paleolatitude which is in turn needed to express a given field value at a site as a dipole moment (i.e., the value needed for eqn 1). To obtain paleointensity, an oriented thin section approach was developed (Tarduno et al., 2007). Application of this technique suggests virtual dipole moments of $3.2 \pm 0.31 \times 10^{22} \text{ A m}^2$ for the Nondweni dacite, and $4.3 \pm 1.0 \times 10^{22} \text{ A m}^2$ for the Barberton dacite. Thus a strong magnetic field was present during a time for which we have the oldest microfossil evidence for life (Wacey et al., 2011). However, what were the details of the shielding environment? Having these magnetic dipole moment constraints, the next step in our quest to calculate magnetopause standoff is to constrain solar wind pressure in the past, as discussed below.

3.3. Solar Wind and magnetopause at 3.45 Ga

The property of the Archean to Hadean Sun that has most captured the attention of the geological community is its luminosity. The Sun began the main sequence phase of its life at a luminosity $\sim 30\%$ lower than the present-day value (Gough, 1981). Because of the conversion of H to He in the Sun’s core, density and temperature increase, and luminosity rises. The “Faint Young Sun Paradox” highlights the expectation that this reduced luminosity should have resulted in a snowball Earth (Sagan and Mullen, 1972), but sediments (including those from the Barberton Greenstone belt) indicate deposition in shallow warm seas.

The solution to the paradox is generally posed in the form of some greenhouse gas concentration in the early Earth’s atmosphere. We will briefly revisit this question later, but for now the variable of greatest interest for addressing equation 1 is not luminosity, but other aspects of the Sun’s radiation, specifically the solar wind (mainly hydrogen ionized to protons), X-rays and energetic

UV radiation. Unlike Earth, where field strength relates to buoyancy forces, the Sun’s magnetic field is a strong function of its rotation rate. The solar dynamo has its origin in the interactions between rotation and its convective outer envelope (Parker, 1970). The Sun sheds angular momentum through the emission of magnetized winds and rotation slows in a process known as magnetic braking. The rotation period slows as $\sim t^{\frac{1}{2}}$ (e.g. Ayres, 1997).

Stellar winds are not detected directly, but through interaction with the interstellar medium. The interaction forms an “astrosphere” surrounding a star created by hot, interstellar neutral hydrogen which is heated by the stellar wind. Hot hydrogen atoms can be detected spectroscopically because they produce an absorption feature (H I Lyman- α) thereby proving an indirect means of gauging stellar winds.

Observational constraints on ancient mass are available from the study of solar analogs - stars that are approximately the same size as the Sun but have different ages (e.g. Wood, 2006). These data suggest that current and past mass loss are related by a power law:

$$\frac{\dot{m}v_{sw}}{\dot{m}_0v_{sw0}} = \left(\frac{t}{t_0}\right)^{-2.33} \quad (6)$$

where \dot{m}_0 , v_{sw0} are the present-day mass loss and solar wind velocity, respectively. As we will discuss later, this relationship should be applied to the Sun only for solar ages greater than ~ 700 million years. This relationship suggests that the solar mass loss at 3.45 Ga was $2.4 \times 10^{-13} M_{\odot}/\text{yr}$, where M_{\odot} is the current solar mass. This mass loss can be used to further derive a model (Model A of Tarduno et al. (2010)) of wind velocity and density change with time, which comprise solar wind pressure. Hence, we can now solve equation 1 to obtain estimates of magnetopause standoff distance as a function of dipole moment (Figure 5).

The paleointensity estimates for 3.4-3.45 Ga from the Kaapvaal Craton dacites suggest standoff distances of ~ 5 Earth radii (R_e). One can also estimate mass loss from rotation and X-ray emission. Stellar evolution models

predict the Sun at 3.45 Ga would appear to be a G6V star having a rotational period of ~ 12 days (Mamajek and Hillenbrand, 2008). Mass loss rates among solar-type stars can be related to X-ray emission (f_X) and rotation as:

$$\dot{m} = \dot{M}_{\odot} \left(\frac{R}{R_{\odot}} \right)^2 \left(\frac{f_X}{f_{X_{\odot}}} \right)^{1.34 \pm 0.18} \quad (7)$$

where R is solar radius, R_{\odot} is the modern value, and $f_{X_{\odot}}$ is the modern soft X-ray surface flux ($\sim 10^{4.57}$ erg/s/cm² in 0.1-2.4 keV band). Equation 7 (Model B of Tarduno et al. (2010)) predicts a higher mass loss of 1.5×10^{-12} M_{\odot} /yr and a smaller standoff of $\sim 4 R_e$. Even using the more conservative mass loss of Model A, the standoff distance is expected to be only $\sim 50\%$ of the present-day value. Sterenborg et al. (2011) presented results of a magnetohydrodynamic numerical simulation of Paleoproterozoic conditions utilizing modules of the Space Weather Modeling Framework (Toth et al., 2005). They obtained standoff distances within error of our estimates, confirming the compressed Paleoproterozoic magnetosphere.

The change in standoff relative to today may in itself seem abstract, but we have a very good idea of what these conditions are like because they are typically experienced during modern events, such as the Halloween solar storms of 2003 (e.g. Rosenqvist et al., 2005). However, during modern events like the Halloween storms, reduced standoffs occur on hour to day timescales. In contrast, these conditions would represent the typical day 3.4 to 3.45 billion years ago. Thus, while the magnetic field was present and provided some shielding from the solar wind, the reduced standoff conditions suggest there nevertheless could have been important modifications of the early Earth's atmosphere. Below, we first provide context through a discussion of atmospheric loss processes.

4. Atmospheric Loss Mechanisms

Atmospheric loss mechanisms are typically divided into thermal escape stimulated by energetic photons and non-thermal escape associated with the interaction of charged particles. Following this classification, the presence/absence of a magnetic field will influence only non-thermal escape. However, thermal processes are also of importance because they determine whether non-thermal loss is likely to be efficient. Moreover, as we introduce below, under reduced standoff conditions of the early Earth, heating due to solar wind interaction with the atmosphere is possible, and in this case the clear-cut assignment of magnetic field influence to only non-thermal processes becomes less meaningful.

Much can be learned about these atmospheric loss processes by study of planets without internally generated magnetic fields, namely Venus and Mars, and the general interest has expanded in parallel with exoplanet discoveries and considerations of habitability (e.g. Seager, 2010). The limitations of these analogies should also be kept in mind; atmospheric loss processes presently working at Venus and Mars are the result of different evolutionary histories of their respective atmospheres. While analogies should not be taken too far, the physical processes are illustrative, notwithstanding the difficult task of deciding the importance of these processes for the young Earth.

4.1. Thermal escape

The uppermost tenuous part of the atmosphere is known as the exosphere; it begins at the exobase, where the mean free path of molecules is so large that collisions before escape are unlikely. In Jeans' escape (Jeans, 1925), a molecule gains sufficient energy to reach its escape velocity. The important Jeans' escape parameter λ_J is defined as the ratio of gravitational potential energy to thermal energy:

$$\lambda_J \equiv GMm/kT_J r_J \quad (8)$$

where, G is the gravitational constant, M is the planetary mass, m is the mass of the escaping particles, k is Boltzmann’s constant, T_J is the temperature of the exobase and r_J is the radius of the exobase. A central parameter in understanding thermal escape in the past is thus knowing the temperature at the exobase, and this in turn will depend of the solar flux, particularly that in the X-ray to energetic ultraviolet (EUV) spectral range (wavelength $\leq 1027 \text{ \AA}$) commonly referred to as XUV radiation. Astrophysical observations of solar analogs (e.g. Dorren and Guinan, 1994) have provided data to constrain the past solar flux. Ribas et al. (2005) define a flux as a function of stellar age (t) as:

$$F = 29.7 t^{-1.23} \text{ ergs s}^{-1} \text{ cm}^{-2} \quad (9)$$

where the flux is defined at wavelengths between 1 and 1200 \AA . At 2.5, 3.45 and 4 Ga, this flux would be about 3, 6, and 13 times greater (respectively) than today. This increased flux has the potential to heat the exosphere (but this also depends on atmospheric composition, see *section 4.3*) and increase ionization, promoting non-thermal escape.

If heating is sufficiently great ($\lambda_J < 1.5$; Opik (1963)) atmospheric “blowoff” can occur. The more general term is hydrodynamic escape, where the thermal energy from XUV radiation allows an escaping species to efficiently stream away from the planet. It is particularly important for hydrogen-rich exospheres, potentially including that of the early Earth (Watson et al., 1981). Hydrodynamic escape will be important only if the supply of the escaping species is not limited by diffusion lower in the atmosphere.

The diffusion limited flux (F_d) can be expressed as (Hunten, 1973):

$$F_d = b \left(\frac{GM}{kT} \right) (m_j - m_i) \left(\frac{n_i}{n_j} \right) \quad (10)$$

where (F_d) is diffusive flux per steradian per second, b is a binary collision parameter, $\mathcal{O} (10^9) \text{ cm}^{-1} \text{ s}^{-1}$, n is number density and the subscripts i and j refer to the escaping and background gas masses, respectively, and n_i/n_j is the

mixing ratio of the escaping gas.

If we consider hydrogen as the gas escaping from a background of nitrogen, mixing ratios greater than a few percent suggest that escape will be energy related rather than diffusion limited (Watson et al., 1981), and this seems likely given the potential sources of hydrogen ranging from dissociation of water vapor to volcanic outgassing. In fact, faced with the likelihood of hydrogen accumulation in a pre-Proterozoic anoxic Earth, the relevant question is one of determining how large amounts of hydrogen were removed such that the atmosphere did not become highly reducing (evidence for which is lacking in Paleoarchean and younger rocks).

Two final aspects of hydrogen hydrodynamic escape are of note. Hydrodynamic escape of hydrogen has the potential to carry out with it heavier atmospheric species. Watson et al. (1981) used equation 10 to predict that heavier species would probably not be removed, with the exception of deuterium. This prediction is consistent with the lack of nitrogen isotope ($^{15}\text{N}/^{14}\text{N}$) fractionation observed on Earth (Marty et al., 2013), versus, for example, that observed on Mars (e.g. Jakosky et al., 1994) where thermal and nonthermal processes have greatly thinned the atmosphere. However, the removal of hydrogen could leave behind excess atmospheric oxygen that would have to be either incorporated into the crust/mantle or lost. Kulikov et al. (2007) suggest oxygen could be lost by hydrodynamic escape given early Earth EUV conditions.

Another type of thermal loss is that associated with large impacts. The Paleoarchean of the Barberton Greenstone Belt (and the Pilbara Craton) contains evidence for large impacts in the form of spherule beds (e.g. Lowe et al., 2003); these may represent the tail of a distribution of large impacts known as late heavy bombardment (Bottke et al., 2012). During a large impact the atmosphere can be super-heated by shock to the point that some is blown-off. We include this process in the discussion because during this heating, non-thermal removal processes will also be enhanced. This effect would be most relevant for times after the main thermal pulse resulting from shock.

4.2. *Non-thermal escape*

Non-thermal processes encompass a wide range of escape mechanisms that are summarized in Table 1. Some of these involve photons (e.g. photodissociation) whereas others involve interaction with the charged solar wind and collectively can be grouped into “solar wind erosion”. Light atmospheric species that have been ionized by EUV photons, charge exchange with solar wind protons, or by impacts with solar wind electrons (Luhmann et al., 1992) can be removed by the solar wind. Ionized light and heavier ions that are not removed can reenter the atmosphere. When they impact neutral species near the exobase, some of the target species will be scattered, gaining enough energy to escape, in a process known as “sputtering”. Heavier species (e.g. N_2^+ , O_2^+) will be more effective as sputtering agents (Johnson, 1990).

Of particular importance for our consideration are those non-thermal processes that involve ion escape, because these generally require open field lines. Ions can also travel along the magnetic field and escape through the magnetotail (e.g. Kistler et al., 2010). Open flux also occurs near the magnetic poles, where magnetic field lines connect with the interplanetary field. The polar cap is defined as the region where open flux occurs and the auroral zone is at its boundary. The solar wind can penetrate deeper into the atmosphere in the polar cap causing ionization, and this is also the region where energetic ions can escape; for example depletion of H and He above the Earth’s magnetic poles today is due to escape along open field lines (de Pater and Lissauer, 2001). Ions can also be lost when reconnection takes place, when the magnetic field of the solar wind joins the terrestrial magnetic field (e.g. Lyon, 2000). This is classically expressed as a southward interplanetary (solar wind) magnetic field connecting with a northward magnetosphere field, and this type of reconnection is pronounced during coronal mass ejection events when magnetized solar plasma impacts the magnetosphere. However, reconnection is a complex phenomena that has been observed under a variety of solar forcing conditions.

Table 1: Atmospheric Escape Processes[†]

Process	Example Reactions	Current Planetary Example	Early Earth [‡]
Charge exchange ¹	$H + H^{+*} \rightarrow H^+ + H^*$ $O + H^{+*} \rightarrow O^+ + H^*$	Earth (H, D) Venus (He)	↑
Dissociative recombination ²	$O_2^+ + e \rightarrow O^* + O^*$ $OH^+ + e \rightarrow O + H^*$	Mars (O) Venus (H), Mars (N)	↑
Impact dissociation ³	$H_2 + e^* \rightarrow H^* + H^*$ $N_2 + e^* \rightarrow N^* + N^*$	Mars (N)	↑
Photodissociation	$O_2 + h\nu \rightarrow O^* + O^*$ $H_2O + h\nu \rightarrow OH^+ + H^*$ $OH^+ + h\nu \rightarrow O + H^*$		↑
Ion-neutral reaction ⁴	$O^+H_2 \rightarrow OH^+ + H^*$		↑
Sputtering or knock-on ⁵	$O^* + H \rightarrow O^* + H^*$	Venus (H)	↑
Solar-wind pickup ⁶	$O + h\nu \rightarrow O^+ + e$ then O^+ picked up	Mercury (He, Ar)	↑ [§]
Ion escape ⁷	H^{+*} escapes	Earth (H,D, He)	↑ [§]
Electric fields ⁸	$X^+ + eV \rightarrow X^{+*}$	Earth (H,He)	↑ [§]
Jeans escape			↑
Hydrodynamic escape			↑
Impact erosion			↑

[†]Adapted from (Hunten et al., 1989; de Pater and Lissauer, 2001; Seager, 2010).

* Excess kinetic energy.

[‡]Referenced at ~ 3.45 Ga for comparison with magnetopause reported in (Tarduno et al., 2010).

↑, ↓, escape greater or lower at ~ 3.45 Ga than today.

↑[§], overall escape greater due to increased ion supply.

¹Charge exchange occurs when an energetic ion collides with a neutral, and the ion loses its charge but retains its kinetic energy. The former ion can have enough kinetic energy to escape.

²Dissociative recombination occurs when an ion dissociates on recombination with an electron, resulting in atoms with sufficient energy to escape.

³Impact dissociation occurs when a neutral molecule is impacted by an electron; the resulting energetic atoms can escape. Similar end products result from photodissociation, but rather than an electron impacted by a molecule, energy is transferred by photons.

⁴Ion and neutral molecule can also react to form an ion and an energetic atom.

⁵When an energetic atom or ion collides with an atmospheric atom, the atom is ac-

celerated and may escape. A single collision is referred to as knock-on. Sputtering describes a cascade of collisions following the initial collision, with these later collisions supplying enough energy for atmospheric escape.

⁶In the absence of an internally generated dynamo field (or in the case of a very weak field), charged atmosphere particles can interact directly with the solar wind and be carried away, in a process known as solar wind pickup or sweeping. If a planet lacks an internal field, but has an atmospheric and an induced magnetic field, particles are picked up at the subsolar point and lost at the tails of the induced magnetosphere.

⁷When magnetic field lines are open, energetic atmospheric ions can escape (ion escape).

⁸Charged particles can be accelerated by electric fields of magnetospheric or ionospheric origin aiding escape as they are lost as they move out along magnetic field lines (associated with either an internal-generated or induced magnetosphere).

4.3. Atmospheric chemistry

The type of loss that is most important at a given time is a function of atmospheric chemistry. Below we focus on a few aspects of this complex topic relevant to our considerations of atmospheric loss on the early Earth and refer readers to the excellent synthesis on planetary atmospheres by Pierrehumbert (2010).

The extent of the atmospheric loss from its top will be dependent on temperature, which in turn depends on whether the dominant species are good or poor infrared emitters (Lammer, 2013). For example, CO_2 is a good infrared emitter; it dominates the exobase of Venus and as a result the temperature is relatively cool (200-300 K). In contrast, atomic O is a poor infrared emitter; it dominates the present exobase of Earth and the temperature is relatively high (1000 K). Nitrogen is neither a good or poor IR-emitter, so the exobase temperature will tend to be controlled by other species (Pierrehumbert, 2010). The question of what these species might be in the early Earth's atmosphere is itself hotly debated, principally focused on the greenhouse gases needed to counter the Faint Young Sun, and the amount to which the atmosphere was reducing (Shaw, 2008).

Proposed solutions to the Faint Young Sun have included increased atmospheric NH_3 (Sagan and Mullen, 1972), CO_2 (Owen et al., 1979), CH_4 (Kiehl and Dickinson, 1987; Catling et al., 2001), or a decreased albedo (Rosing et al., 2010). Various counterarguments have been made (see comprehensive review by Feulner (2012)). NH_3 should be quickly dissociated by photolysis; its survival was postulated because of the sheltering effect of a hypothetical thick Titan-like organic haze layer resulting from photolysis of CH_4 . However, a haze layer can have a cooling effect (Haqq-Misra et al., 2008). Nevertheless, an optically thin haze layer might be an effective UV screen (Hasenkopf et al., 2011). The ratio of the mixed valence state magnetite to siderite in banded iron formations (BIFs) appears to limit atmospheric CO_2 levels (Rosing et al., 2010), but this strictly applied to the oldest well-preserved Archean BIFs. Moreover, this apparent limitation relies on the assumption that iron mineral formation in BIFS was not far from equilibrium with the atmosphere; this assumption has been questioned (Dauphas and Kasting, 2011; Reinhard and Planavsky, 2011). Goldblatt and Zahnle (2011) argue that albedo effects alone cannot resolve the Faint Young Sun Paradox to a factor of 2 of the needed radiative forcing (but see also responses by Rosing et al. (2011)). Nitrogen itself, while not a greenhouse gas, could have aided early greenhouse warming because its presence broadens the absorption lines of other greenhouse gases (Goldblatt et al., 2009).

Notwithstanding the continuing debates, a $\text{N}_2\text{-CO}_2$ atmosphere, with important time dependent roles for hydrogen and methane, seems to be the closest consensus available for the early Earth. The importance of methane likely tracks the start of its production biologically (Catling et al., 2001), whereas the very early presence of hydrogen in the atmosphere seems unavoidable given early high degassing rates, although concentrations are also debated (Tian et al., 2005; Catling, 2006). Several authors have noted that the removal of hydrogen by thermal and non-thermal processes could have contributed to the change from a reducing to oxidizing atmosphere (Catling et al., 2001; Lammer et al., 2008). We recall that loss of this hydrogen can adiabatically cool the exosphere, limiting loss of heavier species (Tian et al., 2008; Lammer, 2013) whereas H_2 -

N₂ collision-induced warming is another mechanism that could counter effects of the Faint Young Sun (Wordsworth and Pierrehumbert, 2013).

There is another potential bottleneck of importance that could control the loss of water from the early Earth. Today, water loss is limited by the cold trap at the top of the troposphere where temperatures are low and water condenses, leaving the stratosphere relatively dry. Given a current loss of H from the atmosphere of 2.7×10^8 atoms cm⁻² s⁻¹, only about 5.7 m of a global ocean on Earth would be removed in 4.5 billion years (Hunten et al., 1989).

Since water vapor is controlled by surface temperature, and Archean surface temperatures are argued to have been temperate (e.g. Blake et al., 2010), there is no reason to suspect the lower atmosphere was unusually dry. However, with the lack of a ozone layer in the anoxic Earth, greater penetration of UV into the atmosphere (causing photolysis of water), and greater UV output of the young Sun, a cold trap may not be as limiting, as has been suggested for the primitive Venusian atmosphere (Chassefiere, 1997). The example of Venus merits further discussion (below) because it and Mars are sometimes offered as examples relevant to the importance of magnetic fields on atmospheric loss.

4.4. The apparent Martian and Venusian counter-examples: issues in assessing the effectiveness of a magnetosphere

While it has been traditionally postulated that the difference between the current water inventory of Earth versus that of Mars is due to the presence of an internally generated magnetic field on the former (e.g. Lundin et al., 2007), there have been several more recent dissenting voices, to the point that some have even questioned the more general importance of a magnetic field (Kasting, 2010) and particularly whether a stronger field could even lead to increased dispersal of the atmosphere (Brain et al., 2013). These issues raised, follow one or more of the following threads of reasoning:

(i) Venus lacks an internal magnetic field but retains a thick atmosphere, providing a circumstance in which seemingly magnetic shielding is unimportant for atmospheric protection, and by extension, habitability.

(ii) The present-day total atmospheric ion escape from Earth, Mars and Venus appears to be within similar orders of magnitude, at 10^{24} - 10^{26} ions s^{-1} (Barabash, 2010; Strangeway et al., 2010). Because Earth has an internal geomagnetic field and Mars and Venus do not, an internal magnetic field must not be that important for water loss/survival.

(iii) Planets with atmospheres have an induced magnetosphere that provides atmospheric protection, therefore a specifically internally generated magnetic field is unnecessary for atmospheric survival.

(iv) Ions can be accelerated and channeled along large scale field lines, particular toward the poles in a large scale dipole configuration. In this respect, by converging the incoming particle flux, the magnetic fields help to exacerbate the atmospheric loss rather than abate it (Brain et al., 2013)

Sorting out the evidence in support of and in opposition to these arguments comprises an important opportunity for further research. Here we discuss each of them a bit further to highlight what we think are particularly important aspects to consider further when critically assessing the role of magnetic fields in atmospheric retention and habitability.

With regard to argument *i*, the distinction between merely retaining an atmosphere vs. the retention of specifically water must be kept in mind. While the exact evolutionary history and escape mechanisms are debatable (e.g. Kasting, 1988; Elkins-Tanton, 2013; Hamano et al., 2013), there is little argument that Venus has lost a huge amount of water relative to Earth. This has irreversibly altered its atmosphere, to the point that the probative value of present-day conditions on Venus for understanding the solar-terrestrial environment of the

early Earth is limited. The present Venusian CO₂ atmosphere has a relatively cool exobase limiting loss. It is true that a magnetic field is not necessary to retain an atmosphere but, the relevant issue for life as we know it is water.

The evolution of a planetary atmosphere is also dependent on the evolution of its host star’s wind. Indeed the fact that the young sun had a stronger solar wind is important in considering argument *ii*, which ignores the greatly enhanced solar winds and XUV radiation environment associated with the rapidly rotating young Sun (*sections 3.3, 4.1* of this paper). In fact the extreme XUV atmospheric heating may have been so great that the exosphere moved beyond the magnetosphere associated with a geodynamo (e.g. Lammer et al., 2008; Tian et al., 2008). In this case, by definition part of the atmosphere will be unprotected by the magnetic field against loss. But atmospheric escape rates could be even higher in such a case in the absence of an internally generated magnetic field, because solar wind protons would more readily gain access to denser parts of the atmosphere. In fact, the question becomes one of atmospheric survival, even given a N₂-CO₂ atmosphere (Lichtenegger et al., 2010). Recent measurements of present-day conditions do show that Mars and Venus have in fact exhibited accelerated atmospheric loss during times of increased solar wind pressure (Edberg et al., 2010, 2011), whereas a direct comparison of Earth and Mars under the same solar forcing found that Martian atmospheric loss was more sensitive to increases in solar wind pressure (Wei et al., 2012), strongly suggesting the importance of the geomagnetic shield.

In assessing the importance of a magnetic field for habitable atmosphere retention, we must in fact distinguish between a field induced externally by wind-atmosphere interactions (argument *iii*) vs. supplied internally via a dynamo. The structure and location of influence of the field would be different in the two cases and this must be considered in comparing the relative influence. As summarized by Brain et al. (2013), the field arising from interactions between the wind (perhaps as in present day Venus, Mars and Titan) likely deflects the wind only within $\lesssim 1$ planetary radii where as in internally produced field could be stronger, and abate the incoming wind at larger radii from the planet.

Because an internally produced magnetic field would be anchored in the core, field lines converge toward magnetic poles. The role of a large magnetosphere combined with convergence of the field toward the poles may indeed be important in assessing the sign of the influence of the magnetic field on atmosphere retention, as suggested in argument *iv*. Because incoming wind ions typically have very small gyro-radii, they are captured onto field lines that are concentrated toward the poles as discussed in Brain et al. (2013). Supporting evidence comes in part from observations Strangeway et al. (2005) of the outward flux of O ions from auroral zones is consistent with concentration of a higher solar wind energy flux by up to 2 orders of magnitude in these regions, and is consistent with theoretical considerations of Moore and Khazanov (2010). Such an effect would preferentially eject heavy ions that would otherwise be gravitational bound at atmospheric temperatures, unlike light ions like H^+ whose thermal speed would already exceed the escape speed.

Despite the plausibility of this magnetically aided concentration of wind flux toward the polar caps, we note that there are a number of effects to keep in mind in assessing its influence on habitable atmosphere retention. First, note that the same magnetic fields that might help concentrate the effect of the solar wind in local regions, also create a magnetospheric environment that can result in recapture. For example, the polar outflow of O^+ from Earth today is some 9 times greater than the net loss, considering recapture in the magnetosphere (Seki et al., 2001). A local outflow might therefore not always result in a catastrophic global outflow. Second, the depth to which ions can be accelerated by conversion of solar wind flux into the accelerating Poynting flux also depends on competing forces such as a magnetic mirror force (Cowley and Lewis, 1990). Converging field lines can reflect particles, and trap them above a certain height. The specific depth to which ions can penetrate may be limited for specific planetary circumstances and should be quantified. Third, the time scale for the full atmosphere of ions essential for habitability to be ejected at local auroral regions depends on how fast the atmosphere can circulate into these regions of loss. This resupply requires horizontal flow to refill the cone of

loss and thermal diffusion to move material up to the exobase. The slower of these mechanisms determines the rate of loss.

While our main purpose here is to provide an introduction to the issues warranting further quantitative study, we now present one calculation on which all influences of the magnetic fields depend, namely the estimate of the impinging rate of solar ions for magnetically shielded versus unshielded planets (Figure 6). Regardless of how the flux that penetrates the atmosphere subsequently evolves, this calculation is the basic starting point for assessing how much stellar wind flux first enters the magnetosphere.

The rate of solar ions with the potential to enter a planet’s atmosphere depends on the product of the effective area onto which ions are captured and the speed of the inflow. A large magnetosphere increases the effective area but reduces the inflow speed at which the ions flow into the atmosphere by abating the ram pressure of the solar wind and compressing the solar wind field at the magnetopause with the solar wind ions kept out. However, when the solar wind and magnetosphere fields reconnect, the solar wind ions can bleed onto the planetary magnetic field and into the atmosphere. The speed at which ions flow into the atmosphere is $\sim 1/2$ the inflow reconnection speed when averaged over time if we assume that the solar wind field orientation is favorable to reconnection $\sim 50\%$ of the time. During the reconnection phase, the effective collecting area of stellar wind ions can become as large as the magnetopause radius (on the daylit side). Keeping these concepts in mind, the mass flux collected by a planet without a magnetosphere \dot{M}_c from a stellar wind whose velocity exceeds the escape speed of the planet at its surface can be written as:

$$\dot{M}_c \simeq \frac{\pi r_p^2}{4\pi R^2} \dot{M}_w \quad (11)$$

where r_p is the planet radius and R is the planet star distance assuming $R \gg r_p$, and \dot{M}_w is the wind mass flux. In the presence of a magnetosphere, the mass

flux collected $\dot{M}_{c,m}$ is given by:

$$\dot{M}_{c,m} \simeq \frac{\pi r_m^2}{4\pi R^2} \frac{v_{rec}/2}{v_{sw}} \dot{M}_w \quad (12)$$

where v_{rec} is the reconnection speed at the magnetopause, v_{sw} is the wind speed, and r_s is the magnetospheric distance from the planet. We have assumed $R \gg r_s$. Taking the ratio of equation 12 to equation 11 gives:

$$Q \equiv \frac{\dot{M}_{c,m}}{\dot{M}_c} \simeq 1.75 \left(\frac{v_{rec}}{25\text{km/s}} \right) \left(\frac{v_{sw}}{400\text{km/s}} \right)^{-1} \left(\frac{r_s/r_p}{10} \right)^2 \quad (13)$$

where we have scaled to the present solar wind- Earth values for reconnection at the magnetopause (Cassak and Shay, 2007; Paschmann et al., 2013; Walsh et al., 2014). Note that the estimate of the reconnection speed at the magnetopause is consistent both with the value estimated theoretically based on asymmetric reconnection (Cassak and Shay, 2007) and observations (Walsh et al., 2014).

While a crude estimate, if we scale equation 13 to Earth at 3.45 Ga when $r_s/r_p \sim 5$ this factor would reduce to 0.43 if v_{rec}/v_{sw} remained the same. Being less than or of order unity, it highlights that despite having a collection area 100 times larger, a robust magnetosphere collects less total ions at r_s than directly impact the atmosphere of an unshielded planet. The fact that Q is not $\ll 1$ implies that the fate of ions trapped at r_s may be an important factor in evaluating the effectiveness of magnetospheric shielding of atmospheres. We should consider the concentration of all of this collected flux onto polar caps covering a surface area fraction A_{cap} at the radius from the planet's center where the ions are stopped, then the total wind flux impinging onto these caps would be $q_{cap} = Q/A_{cap}$. Today q_{cap} is $\gg 1$ because $A_{cap} \ll 1$. However, we recall that observations indicate that atmospheric loss from Earth is not much greater than that at Mars (which presently lacks an internal dynamo), contrary to that predicted if the focusing effect was the dominant factor in atmospheric loss. One reason for limited loss may be the return of ions in the magnetotail. It may be that increases in focusing at the polar cap associated

with a magnetosphere are balanced by increased trapping in the magnetotail. For the early Earth, we cannot assume $A_{cap} \ll 1$, as discussed below.

4.5. Implications for atmospheric escape at 3.4 to 3.45 Ga

While the Paleoproterozoic geodynamo produced a magnetic field that probably prevented whole-scale removal, magnetic field and solar wind strengths suggest important modifications of the atmosphere by thermal and non-thermal escape processes during the first billion years of Earth evolution. The ~ 6 times greater XUV flux relative to today would have heated the exosphere to many thousand Kelvin, promoting thermal loss of hydrogen. The reduced standoff conditions would allow greater interaction of solar wind protons with the extended atmosphere, exacerbating thermal loss with non-thermal loss mechanisms (Table 1). The reduced standoff conditions would also be associated with expansion of the polar cap, that area where open field lines allow access of the solar wind to the deeper atmosphere. Tarduno et al. (2010) used the latitude of the aurora to estimate the polar cap area derived from a scaling law of Siscoe and Chen (Siscoe and Chen, 1975):

$$\cos \lambda_p = \left(\frac{M_E}{M_{E_0}} \right)^{-1/6} P^{1/12} \cos \lambda_{p_0} \quad (14)$$

where λ_p is the magnetic latitude of the polar cap edge, λ_{p_0} is the present-day value of 71.9° , M_{E_0} is the present-day dipole moment, and P is the solar wind dynamic pressure normalized to the present-day value (~ 2 nPa). Using this scaling law, Tarduno et al. (2010) suggested the polar cap could have increased by as much as a factor of 3 under Paleoproterozoic solar wind forcing. In numerical simulations using the Space Weathering Modeling Framework modules, Sterenborg et al. (2011) also found polar cap enlargements, but by smaller amounts (15-50%). We note that the larger values reflected the most compressed magnetospheres (model B) which represent much smaller standoff distances than those obtained in the simulations. Equation 14 assumes a circular polar cap; day-night side asymmetry should modify this shape, and the simulation results

show highly elliptical polar caps. The circular approximation may be a better estimate of the open flux area sampled during one day.

The combined effect of enhanced XUV, reduced magnetic magnetopause standoff, and increased polar cap area would have promoted the loss of hydrogen and ultimately water from the Paleoarchean Earth. The limiting factor for the water loss was probably not conditions of the upper atmosphere, but the efficiency of water transport through a lower atmosphere cold trap. However, high rates of photolysis related to the large Paleoarchean UV flux may have enhanced the net removal of water. Given that these reduced standoffs existed for hundreds of millions of years (Figure 5), water transport and removal is probable. This in turn implies that the Earth may have had a greater water inventory at and prior to the Paleoarchean, allowing for preservation of the modern oceans. The gradual removal of hydrogen under reduced standoff conditions may also have been important for the transformation of Earth’s atmosphere from one that was mildly reducing to one that was oxidizing.

The near certainty of extreme heating causing expansion of the atmosphere prior to 3.45 Ga, and creating even greater opportunities for atmospheric escape provides motivation for determining solar-terrestrial interaction for even older times. We start with a discussion of recent model predictions of dynamo onset, follow this with estimates of solar winds for the first 700 million years of Earth, and conclude with a discussion of the potential for magnetic field strength observations for times $\gg 3.45$ Ga.

5. Delayed Dynamo Onset

While the paleointensity values at 3.4 to 3.45 Ga are slightly less than present-day, they are not remarkably different from variations that may have occurred over the last 200 million years (e.g. Aubert et al., 2010). This raises the question of whether Earth has always had a relatively strong magnetic field, dating from a time shortly after core formation. Several diverse lines of reason-

ing have been used to argue otherwise, with dynamo onset extending to times just older than the 3.45 Ga constraint discussed above. *Notwithstanding caveats discussed in section 4.4*, a delayed dynamo onset and its associated long period without magnetic shielding imply a correspondingly long episode of extreme water loss. In this case, a huge initial water reservoir and/or large supply as a late veneer (e.g. Albarede, 2009) may be needed to account for the present-day conditions.

One of the most fascinating of these delayed dynamo hypotheses is derived not from the study of terrestrial samples, but from investigations of the Moon. Lunar ilmenite samples obtained during Apollo missions have unusual nitrogen isotopic values; these have been interpreted by Ozima et al. (2005) as reflecting nitrogen picked up from Earth’s atmosphere by the ancient solar wind and transported to the lunar surface. An example of this process is the pickup of elements from Venus observed today. The relevant point for our consideration is that Ozima et al. (2005) recognized the importance of magnetic shielding and hypothesized that the Earth’s magnetic field was null (or of very low intensity) during the time of nitrogen transfer, which was constrained by the age of the Apollo samples (3.9 to 3.8 Ga). On the basis of terrestrial constraints, this remains a viable hypothesis.

However, emerging paleointensity from lunar samples suggest an important component of magnetic shielding may have been present on the Moon. The Moon appears to have a core that is at least partially molten (Weber et al., 2011) and magnetized crust (Carley et al., 2012), and it has long been suspected that an ancient dynamo was once present on the basis of analyses of Apollo samples (Fuller and Cisowski, 1987). The fidelity of paleointensity data from lunar samples is subject to similar domain state constraints as discussed earlier for terrestrial samples, but these limitations pale in comparison to greater obstacles: the inherent thermal instability of FeNi phases that makeup typical lunar magnetic grain populations and the effects of impact-induced shock (Fuller, 1974). Because of the thermal instability, alternating field demagnetization and normalization with applied fields has generally been used to estimate paleointensity

rather than Thellier analyses. Although there have been calibration efforts (e.g. Gattacceca and Rochette, 2004), the accuracy of these data is difficult to assess (see Lawrence et al., 2008) because the laboratory method employed does not replicate the magnetization process. Notwithstanding these uncertainties, recent studies have provided evidence for lunar magnetizations ~ 4.2 billion-years-old (Garrick-Bethell et al., 2009), and possibly extending as young as 3.65 Ga (Shea et al., 2012; Suavet et al., 2013). Beyond the issue of measurement fidelity, the latter interpretations are somewhat controversial because they call for a lunar field at times younger than the time interval predicted for a viable dynamo powered by thermochemical convection (Stegman et al., 2003). However, other dynamo mechanisms, such as impact-stirring (Le Bars et al., 2011) and precession (Tilgner, 2005; Dwyer et al., 2011) might have powered a late lunar dynamo. If confirmed, however, these late lunar magnetic fields pose a serious challenge to the Ozima et al. (2005) hypothesis. (To test his hypothesis, Ozima et al. (2008) have proposed sampling the dark side of the Moon.)

An entirely different approach to constraining the early dynamo history is inspired by the detection of ultra-low seismic velocity zones above the core, interpreted as dense melt lenses (Williams and Garnero, 1996). Labrosse et al. (2007) interpreted these zones as remnants of a once continuous dense melt layer. While present as a continuous layer, Labrosse et al. (2007) postulated that it would form a thermal boundary layer, limiting heat flow from the core and thus suppressing thermal convection needed for dynamo generation. The dense layer was thought to have dispersed into pods sometime between 4 and 3.4 Ga, after which a dynamo could be generated.

Aubert et al. (2010) expressed dynamo evolution in terms of scaling laws derived from numerical simulations and present-day heat flow at the core mantle boundary. In one model, a low CMB heat flow of 3 TW is assumed. This model predicts the presence of an earliest Paleoarchean and Hadean dynamo producing a field comparable in strength to today (Figure 3). A deficiency of the model, however, is that it underestimates modern field values. In another end member, Aubert et al. (2010) considered a CMB heatflow similar of 11 TW; this is closer

to some estimates based on seismology (Lay et al., 2008). In this model, dynamo onset is again delayed to times between 4 and 3.5 Ga.

The Labrosse et al. (2007) and Aubert et al. (2010) high CMB heatflow models are just two in a class of thermal models that suggest the onset of the dynamo may have been delayed because of mantle conditions (Jackson and Jellinek, 2013): the mantle controls heat flow from the core and if the lower mantle is too hot the heat flow will be limited (and the core could theoretically heat up as has been proposed for small bodies). The problem for early dynamo generation has been exacerbated by recent changes in ideas on core thermal conductivity (e.g. Olson, 2013). Hence, onset of the dynamo is naturally linked with the thermal regime of the lowermost mantle, and finding constraints on the dynamo implicitly tells us about mantle history. We will return to the potential for obtaining this record, but first we address extending the solar wind to times older than 3.45 Ga.

6. Solar Wind before 3.45 Ga

In the prior considerations (equations 6-7), mass loss calculations were not extended to the first ~ 700 million years of Earth history. If we were to extend these loss rates to earliest times, it would imply that the Sun was at least a few percent more massive than otherwise assumed in standard models of solar evolution. A greater luminosity associated with this more massive Sun could provide a solution to the Faint Young Sun Paradox (e.g. Sackmann and Boothroyd, 2003).

However, while there are only a few solar analogs for times older than 3.45 Ga whose mass loss is constrained by H I Lyman- α observations (e.g. Wood et al., 2005, 2014), the few that are available seem to define mass loss rates that deviate from the trend defined by older stars. This suggests that there may be a different magnetic topology affecting mass loss. Specifically, the surfaces of very young, active solar-like stars are thought to be dominated by closed magnetic

flux tubes (e.g. Schrijver and Aschwanden, 2002), whereas mass loss mainly proceeds through open flux tubes (e.g. Vidotto et al., 2009). We thus proceed assuming that the few stellar analogs available are suggesting a different solar evolution that must be addressed.

Suzuki (2012) proposed a model which addresses this issue, offering a scenario where the distribution of open magnetic flux tubes important for mass loss for solar-like star evolves with time. Closed flux loops dominate in the youngest times, limiting mass loss even though stellar magnetic field intensity is high. Later, open flux tubes occupy a greater portion of the solar surface. Eventually the mass loss decreases with stellar magnetic field intensity decrease. Suzuki et al. (2013) quantified this scenario as follows:

$$\dot{m} = \dot{M}_{\odot} \left(\frac{c_M}{0.023} \right) \left(\frac{R}{R_{\odot}} \right)^3 \left(\frac{M}{M_{\odot}} \right)^{-1} \left(\frac{\rho_o}{10^{-7} \text{ g cm}^{-3}} \right) \left(\frac{B_{r,0} f_0}{1.25 \text{ G}} \right) \left\langle \left(\frac{\delta v_0}{1.34 \text{ km s}^{-1}} \right)^2 \right\rangle \quad (15)$$

where \dot{M}_{\odot} is the modern solar mass loss rate via wind ($\sim 2 \times 10^{-14} M_{\odot} \text{ yr}^{-1}$), c_M is a conversion factor (numerical simulations suggest ~ 0.02), R is the stellar radius, M is the stellar mass, ρ_o is density (i.e. at the photosphere), $B_{r,0}$ is radial magnetic field, f_0 is the open flux tube filling factor over the photosphere, and δv_0 is a velocity perturbation (which is expected to be a fraction of the sound speed at the photosphere).

Suzuki et al. (2013) ran a series of magnetohydrodynamical simulations of stellar mass loss, varying the input parameters previously discussed over ranges of plausible values. They fit a power-law to their simulation results for X-ray surface flux $f_X < 10^6 \text{ erg cm}^{-2} \text{ s}^{-1}$, in the regime where the kinetic energy of the winds are unsaturated. This X-ray surface flux f_X corresponds approximately to that of the Sun at age $\sim 0.5 \text{ Gyr}$ ($\sim 4.1 \text{ Ga}$), as estimated using the rotational and X-ray evolution relations of Mamajek and Hillenbrand (2008).

We adopt the power-law fits from Suzuki et al. (2013, ; their Equation 25); and scale to an adopted mean modern solar soft X-ray surface flux of $f_{X,\odot} = 3.7 \times 10^4 \text{ erg cm}^{-2} \text{ s}^{-1}$ (based on discussion in Judge et al., 2003, we adopt a

modern-day solar luminosity of $L_X \simeq 10^{27.35} \text{ erg s}^{-1}$), to estimate mass loss and ram pressure as:

$$\dot{m} = \dot{M}_\odot \left(\frac{R}{R_\odot} \right)^2 \left(\frac{F_X}{3.7 \times 10^4 \text{ erg cm}^{-2} \text{ s}^{-1}} \right)^{0.82} \quad (16)$$

$$P_{\text{SW}\odot} = (2 \text{ nPa}) \left(\frac{R}{R_\odot} \right)^2 \left(\frac{F_X}{3.7 \times 10^4 \text{ erg cm}^{-2} \text{ s}^{-1}} \right)^{0.70} \quad (17)$$

where again the modern average solar mass loss is $\dot{M}_\odot \sim 2 \times 10^{-14} \text{ M}_\odot \text{ yr}^{-1}$. The pressure P_{SW} is evaluated at 1 AU, where we scale it to a mean solar wind ram pressure of 2 nPa (based on four decades of measurements compiled at <http://omniweb.gsfc.nasa.gov/html> and commensurate with a mean solar wind density of 7 cm^{-3} and velocity of 440 km s^{-1} . Taking into account the expansion of the Sun over its main sequence evolution, and its empirically constrained rotational braking and X-ray luminosity evolution (Mamajek and Hillenbrand, 2008) we use these scaling relations based on Suzuki et al. (2013) to estimate the mean solar mass loss and solar wind pressure at 1 AU as a function of age.

At age 0.5 Gyr ($\sim 4.1 \text{ Ga}$), these relations predict both a solar mass loss ($\sim 10^{-12.7} \text{ M}_\odot \text{ yr}^{-1}$) and solar wind pressure at 1 AU ($\sim 17 \text{ nPa}$) enhanced over current mean values by only an order of magnitude (Model C, Figure 7; *see also Supplementary Content for further description*). A limitation of this model is that it somewhat underestimates the present-day standoff (Model C: $\sim 9.5 R_E$ vs. present-day value of $10.1 R_E$; Shue et al., 1997).

Moreover, it should be emphasized that priority should be given to additional observations as mass loss during the first 500 million years of Earth history is constrained by analogy with data from only the following 4 stars: $\pi^1 \text{ UMa}$, $\xi \text{ Boo A}$, Proxima Centauri, and EV Lac (Wood et al., 2014). Of these, Prox Cen and EV Lac are active M dwarfs, and $\xi \text{ Boo}$ is part of a binary system where it is not possible to accurately determine the relative contribution of winds from the components. Thus far, there seems to be a “Wind Dividing Line” for stars with X-ray surface flux $> 10^6 \text{ ergs cm}^{-2} \text{ s}^{-1}$ (Wood et al., 2014),

suggesting that our Sun's mass loss during the main sequence stage may have peaked at $\sim 10^{-12} \text{ M}_\odot \text{ yr}^{-1}$ near age $\sim 500 \text{ Myr}$ (4.1 Gya), and been surprisingly lower (only $\sim 0.5\text{-}10\times$ current \dot{M}_\odot) at earlier ages.

Finally, we note that the above calculations have assumed that the relevant pressure associated with inertia of the solar wind is dominated by ram pressure with the solar wind magnetic pressure being subdominant. This is a good approximation for the present sun but a faster rotation and stronger field at the surface of the young sun could increase importance of the magnetic contribution to the solar wind pressure. To see this, note that the strength of toroidal magnetic field that arises from winding up of the poloidal field is given by

$$B_{IMF} = B(r) = B_0 \frac{\omega}{v_{sw}} \frac{r_0^2}{r} \quad (18)$$

where r is distance from Sun, r_0 is solar radius, B_0 is open mean field at solar surface, ω is solar rotation speed (faster for young sun) v_{sw} is solar wind speed. If we ignore the thermal pressure, the total solar wind pressure at a given distance from the sun would then be the sum of the ram + magnetic pressure at that distance, and is then given by

$$\rho_{sw} v_{sw}^2 \left(1 + \frac{B_{IMF}^2 / 8\pi}{\rho_{sw} v_{sw}^2} \right) = \rho_{sw} v_{sw}^2 \left[1 + \frac{B_0^2 \omega^2 r_0^4}{8\pi \rho_{sw} v_{sw}^4 r^2} \right], \quad (19)$$

using equation 18. Using the numerical values appropriate for the present sun of $B_0 = 2\text{G}$, $\omega = 3 \times 10^{-6} \text{ rad/s}$, $r_0 = 7 \times 10^{10} \text{ cm}$, $r = 1.5 \times 10^{13} \text{ cm}$, $\rho_{sw} = 10^{-23} \text{ g/cm}^3$, and $v_{sw} = 4 \times 10^7 \text{ cm/s}$, the magnetic correction term in parenthesis of equation 18 is 0.006 today. If however ω and B_0 were significantly larger at early times compared to the increase in $\rho_{sw} v_{sw}^4$ at early times, then the magnetic correction term could increase. But depending on the mechanism that drives the solar wind, $\rho_{sw} v_{sw}^4$ itself could depend on B_0 and ω so it is also possible that this correct term does not substantially increase. A detailed discussion of these subtleties are beyond the present scope.

7. External source of field for a planet lacking a core dynamo

Given the increased solar wind pressure associated with the young Sun, it is prudent to revisit the question of solar-induced magnetic fields. This is relevant for gauging the minimum field that might be expected in the absence of a early internally-generated dynamo magnetic field for Earth. A lower limit for the external magnetic field is that due to the solar wind itself, and is given by equation 18 which suggests a value between about 7 and 10 nT for Earth today. However, when the supersonic solar wind impacts the atmosphere, field lines are compressed, and an enhancement of the field is expected. The maximum field strength would correspond to the case in which all of the wind ram pressure is converted into magnetic pressure, that is

$$\frac{B^2}{8\pi} \sim \rho_{sw} v_{sw}^2 \quad (20)$$

where ρ_{sw} is the solar wind density. Such equipartition would give a maximum field of about 60 nT today (if Earth lacked an internal magnetic field). This field estimate thus scales with the square root of the solar wind ram pressure. For solar wind pressures of 100 to 1000 times those of today this estimate of the external field would give 0.6 to 2 μ T. We note that for Model C, these values are approached in steady state only for times >4.5 Ga.

The field will would begin to be amplified near the exobase as field lines are compressed, and deeper in the atmosphere as the field lines slip through atmospheric material. The amplified field lines will drape around Earth from the force for the continuous solar wind. The mixing may also be contemporaneous with turbulence that produces complex directional changes in the field on small scales. However, because the solar wind properties vary on such a large scale compared to that of the distance from exobase to Earth's surface, the overall magnitude of the supply energy and spatially averaged field are not expected to vary greatly over the daylight side of the planet. Thus, while there will be overall magnitude variability on day time-scales, a small external field could be sensed by a slowly cooled magnetic mineral on Earth's surface. This serves

as a bound on what paleomagnetic studies might be able to resolve about the earliest core dynamo. We also note that this external field could also serve as a seed-field for the start-up of a core dynamo if it penetrates all the way to the core.

8. Paleoarchean and Hadean Magnetic Sands

Are there rocks that can be sampled to extend the paleointensity record back in time, before 3.45 Ga? The Pilbara Craton of Western Australia hosts Paleoarchean greenschist facies rocks, but these can extend the record from Barberton by only a few tens-of-millions of years. The key time interval for testing the geodynamo presence/absence question is considerably older (cf. Figure 3).

Unfortunately, other terrestrial rocks with ages $\gg 3.45$ Ga have been multiply deformed and metamorphosed to amphibolite-facies (or higher); the thermal and associated chemical transformations remove these from further paleomagnetic considerations. This includes the oldest known rocks, including parts of the 4.03 Ga Acasta Gneiss of northwestern Canada (Bowring and Williams, 1999).

However, there is another recorder: silicate crystals hosting magnetic inclusions that have eroded from primary igneous rocks and are now found in younger sedimentary units. The benefit of this approach is that it might allow us to sample time intervals that are not otherwise available because the original igneous rocks have been lost to erosion. This requires dating of the silicate crystal itself, something that is commonly done with some sedimentary components (e.g. zircons). We note that in using this approach paleolatitudes will typically not be available, because as sedimentary detritus, the orientation of a given silicate crystal relative to horizontal is lost. In this case, inferences on the nature of the global field strength will be limited to the factor of 2 variation of a dipole with latitude. Nevertheless, this is sufficient to test the presence/absence of the geodynamo. We describe approaches to the paleointensity investigation of sili-

ates found in younger sedimentary units below, focusing on what is arguably the most famous unit, the Jack Hills metaconglomerate.

8.1. *Jack Hills Metaconglomerate*

The Jack Hills metaconglomerate is located on the northern edge of the Yilgarn Craton of Western Australia. The unit is rich in zircons and in places, most notable the “Discovery outcrop”, up to 12% of the zircons have ages of 4 billion years or older (Compston and Pidgeon, 1986). The oldest zircons are dated to ~ 4.4 Ga, only some 150 million years after formation of the planet (Wilde et al., 2001). The observation of elevated $\delta^{18}\text{O}$ in some zircons indicates the incorporation of hydrated rocks in magmas from which they grew. This in turn suggests that Earth had oceans at this time (e.g. Cavosie et al., 2007). Because water is an essential ingredient for life as we know it, this observation has motivated some to suggest that the Archean/Hadean boundary should be moved from the traditional age of 3.9 Ga to 4.2 Ga (Valley, 2006). Concerned efforts to find the source of the zircons have failed, leading to the conclusion that these have been lost to erosion, possibly during intense chemical weathering, as supported by $\delta^7\text{Li}$ data (Ushikubo et al., 2008).

The Jack Hills sediments have experienced peak metamorphism of 420 to 475 °C (Rasmussen et al., 2010) and then have been deformed (Spaggiari, 2007; Spaggiari et al., 2007) into a stretched pebble conglomerate. As in the studies on the 3.45 Ga dacites from the Barberton Greenstone Belt, a first step in assessing the viability of the Jack Hills sediments is to conduct a paleomagnetic conglomerate test.

To address the deformation issue, Tarduno and Cottrell (2013) sampled the interiors of cobble-sized rounded clasts, following the idea that they may have primarily undergone rolling motion rather than stretching, limiting penetrative deformation. Magnetic susceptibility versus temperature data indicate the presence of the Verwey transition, the cubic to monoclinic change in the crystal structure of magnetic seen on cooling through 120 K (Verwey, 1939). Thermal

demagnetization reveal a complex series of magnetizations removed at low to intermediate temperatures. Some of these magnetizations are grouped, indicating the potential of magnetization during one of the Archean to Proterozoic metamorphic events that affected the Jack Hills. At relatively high unblocking temperatures, often greater than 550 °C, a distinct component trending to the origin of orthogonal vector plots of the magnetization is commonly observed. This component is scattered, and statistical tests indicate formal passage of the conglomerate test (Figure 8).

This indicates magnetization of the interior part of the cobble only prior to the deposition of the conglomerate; unlike the case of the dacite conglomerate of the Barberton Greenstone Belt, a substantial time period elapsed between the deposition of the conglomerate and the potential age of the mineral components. Most of the Jack Hills sediments appear to have been deposited at ca. 3 Ga, but rare younger units (as young as 1.2 Ga) have been tectonically interleaved. Notwithstanding the potential for some Proterozoic ages associated with these tectonic slivers, it appears that select components of the Jack Hills metasediments have the potential to preserve magnetizations at least as old as ca. 3 Ga.

8.2. *Quartz and Zircon carriers*

Is there a 4 billion-year-old (or older) rock preserved as a clast in the Jack Hills metaconglomerate? The intense chemical weathering called upon for the Hadean would seem to suggest this is unlikely, but it more possible that individual quartz grains composing the Jack Hills clasts are of this age. As discussed above, these quartz grains commonly contain magnetite, and thus they are viable paleomagnetic recorders. However, determining the age of these quartz grains is difficult. In the Jack Hills metaconglomerates, quartz grains often contain zircon inclusions; hence these could provide some age constraints.

Zircon having magnetic inclusions is itself a potential paleomagnetic recorder (hinted at in Dunlop and Özdemir (1997) and discussed explicitly in Tarduno

(2009) and Nelson et al. (2010)), although one that challenges paleomagnetic measurement technology because of their small size (typically <300 microns) and related small number of magnetic included particles. However, high resolution 3-component DC SQUID magnetometers have been used to detect paleointensities from single zircon crystals using Thellier-Coe techniques (Cottrell et al., 2013). It should also be kept in mind that the thermal history of these grains from their formation to their final incorporation into a conglomerate, may not be straightforward. Radiometric age dating coupled with petrologic examinations (i.e. the presence of overgrowths) has the potential to distinguish zircons which may record paleomagnetic signals dating from their initial formations to those that have been reset due to reheating (at times much older than the conglomerate age).

While retrieving a paleomagnetic history from such zircons is a goal, it should be remembered that the complications of zircon resetting are somewhat less important when viewed in the context of simple field absence/presence criteria. That is, the possibility of a “false positive” identification of the geomagnetic field for times older than 3.45 Ga is omnipresent because of subsequent geological activity. But the identification of an anomalously low or null field (within the bounds of recording zero discussed above), if this existed before 3.45 Ga, would be otherwise difficult to explain because of the abundance of opportunities for later magnetization.

9. Summary and Future Potential

The “habitable zone” is classically defined as that distance from a star where liquid water can exist. Even given birth of a planet in this zone, there is no assurance that a habitable planet will evolve given the potential for water loss. The magnetic field is a key factor that must be considered in determining whether a terrestrial-like planet will retain its water. The preservation potential will in turn depend on the balance of stellar wind pressure and magnetic field strength.

Stellar wind history will be a function of star spin rate and stellar evolution. For terrestrial-like planets, salient variables include the time of onset and duration of the dynamo (which are related to the efficiency of heat removal from the core), especially during the first billion years after planet formation.

The magnetic field has competing effects with respect to atmospheric retention (and ultimately water survival). Understanding better the net influence of these effects is itself an important direction of future research. For example, an increased magnetic field provides more pressure to abate the solar wind dynamic pressure and increase the magnetopause radius but the larger magnetopause also means a larger collecting area for solar wind flux during phases of magnetic reconnection. In addition, a strong ordered dipole magnetic field may provide a pathway for concentrating the solar wind flux toward polar caps where its local mass-loss effects may be exacerbated. Yet, this same ordered field provides the magnetic topology for recapturing this mass in the opposite hemisphere such that the net global atmospheric mass loss might not be affected. Comparing similarities and differences of mass loss from planets within our present day solar system will be helpful for progress. Presently available data support the net atmospheric protective role of dynamo magnetic fields.

Ultimately, understanding differences between present-day and early solar wind conditions and influences on Earth's atmosphere (and the atmospheres of other terrestrial planets) is an important goal. To constrain early solar winds, additional observations on solar analog stars younger than 500 Myr (4.1 Ga) are needed. For the Paleoarchean Earth (at ca. 3.4-3.45 Ga), the balance between core dynamo field values and increased solar wind pressure results in standoff of the solar wind to distances half of those of the present-day, suggesting some atmospheric loss and removal of water. This erosive potential implies a more water-rich initial Earth, and/or the delivery of water as a late veneer, to account for the present terrestrial reservoir. The need for large early water reservoirs, or late replenishment, is exacerbated if onset of the geodynamo was delayed by a hot lower mantle. Therefore, from a deep Earth perspective, better constraints on Hadean lower mantle evolution and its interplay with core heat loss could

aid our understanding of the geodynamo/shielding history. These linkages between the early mantle, core dynamo and atmospheric development are equally relevant for Mars (and possibly Venus). From an observational perspective on Earth, there is potential in early Archean and Hadean zircons (and other sedimentary crystals) hosting magnetic inclusions to record the first billion years of the geodynamo using single crystal paleointensity methods. This remains a grand challenge, requiring the most sensitive magnetometers and the development of methods to understand the effects of geologic history after zircon formation. Many of these ongoing instrument and technique developments will have continued application in the analysis of Martian rocks retrieved by future sample return missions.

10. Acknowledgements

We thank Rory Cottrell, Richard Bono, Axel Hofmann, Ariel Anbar and David Sibeck for helpful conversations, and the editor and two anonymous reviewers for their comments. EGB acknowledges partial support from the Simons Foundation. This work was supported by NSF.

References

- Albarede, F., 2009. Volatile accretion history of the terrestrial planets and dynamic implications. *Nature* 461, 1227–1233. doi:{10.1038/nature08477}.
- Amelin, Y., Kaltenbach, A., Iizuka, T., Stirling, C.H., Ireland, T.R., Petaev, M., Jacobsen, S.B., 2010. U-Pb chronology of the Solar System’s oldest solids with variable $^{238}\text{U}/^{235}\text{U}$. *Earth and Planetary Science Letters* 300, 343–350. doi:10.1016/j.epsl.2010.10.015.
- Aubert, J., Tarduno, J.A., Johnson, C.L., 2010. Observations and models of the long-term evolution of Earth’s magnetic field. *Space Science Reviews* 155,

- 337–370. doi:{10.1007/s11214-010-9684-5}. Workshop on Space Science Research of International Space Science Institute (ISSI), Bern, SWITZERLAND, MAR 09-13, 2009.
- Ayres, T.R., 1997. Evolution of the solar ionizing flux. *J. Geophys. Res.* 102, 1641–1651.
- Barabash, S., 2010. Venus, Earth, Mars: Comparative ion escape rates, in: EGU General Assembly Conference Abstracts, p. 5308.
- Biggin, A.J., Strik, G.H.M.A., Langereis, C.G., 2008. Evidence for a very-long-term trend in geomagnetic secular variation. *Nature Geoscience* 1, 395–398. doi:{10.1038/ngeo181}.
- Biggin, A.J., de Wit, M.J., Langereis, C.G., Zegers, T.E., Voute, S., Dekkers, M.J., Drost, K., 2011. Palaeomagnetism of Archaean rocks of the Onverwacht Group, Barberton Greenstone Belt (southern Africa): Evidence for a stable and potentially reversing geomagnetic field at ca. 3.5 Ga. *Earth and Planetary Science Letters* 302, 314–328. doi:{10.1016/j.epsl.2010.12.024}.
- Blake, R.E., Chang, S.J., Lepland, A., 2010. Phosphate oxygen isotopic evidence for a temperate and biologically active Archaean ocean. *Nature* 464, 1029–U89. doi:{10.1038/nature08952}.
- Bottke, W.F., Vokrouhlicky, D., Minton, D., Nesvorny, D., Morbidelli, A., Brasser, R., Simonson, B., Levison, H.F., 2012. An Archaean heavy bombardment from a destabilized extension of the asteroid belt. *Nature* 485, 78–81. doi:{10.1038/nature10967}.
- Bouvier, A., Wadhwa, M., 2010. The age of the Solar System redefined by the oldest Pb-Pb age of a meteoritic inclusion. *Nature Geoscience* 3, 637–641. doi:10.1038/ngeo941.
- Bowring, S.A., Williams, I.S., 1999. Priscoan (4.00-4.03 Ga) orthogneisses from northwestern Canada. *Contributions to Mineralogy and Petrology* 134, 3–16. doi:{10.1007/s004100050465}.

- Brain, D., Leblanc, F., Luhmann, J., Moore, T., Tian, F., 2013. Planetary Magnetic Fields and Climate Evolution. Univ. of Arizona, Tucson. chapter Comparative Climatology of Terrestrial Planets. Space Science Series, pp. 487–501.
- Bressan, A., Marigo, P., Girardi, L., Salasnich, B., Dal Cero, C., Rubele, S., Nanni, A., 2012. PARSEC: stellar tracks and isochrones with the PAdova and TRieste Stellar Evolution Code. MNRAS 427, 127–145. doi:10.1111/j.1365-2966.2012.21948.x, arXiv:1208.4498.
- Caffau, E., Ludwig, H.G., Steffen, M., Freytag, B., Bonifacio, P., 2011. Solar Chemical Abundances Determined with a CO5BOLD 3D Model Atmosphere. Solar Physics 268, 255–269. doi:10.1007/s11207-010-9541-4, arXiv:1003.1190.
- Carley, R.A., Whaler, K.A., Purucker, M.E., Halekas, J.S., 2012. Magnetization of the lunar crust. Journal of Geophysical Research-Planets 117, E08001. doi:{10.1029/2011JE003944}.
- Cassak, P.A., Shay, M.A., 2007. Scaling of asymmetric magnetic reconnection: General theory and collisional simulations. Physics of Plasmas 14, 102114. doi:10.1063/1.2795630.
- Catling, D.C., 2006. Comment on "A hydrogen-rich early Earth atmosphere". Science 311, 38.
- Catling, D.C., Zahnle, K.J., McKay, C.P., 2001. Biogenic methane, hydrogen escape, and the irreversible oxidation of early Earth. Science 293, 839–843. doi:{10.1126/science.1061976}.
- Cavosie, A.J., Valley, J.W., Wilde, S.A., 2007. The oldest terrestrial mineral record: a review of 4400 to 3900 ma detrital zircons from Jack Hills, Western Australia. Developments in Precambrian Geology 15, 91–111.
- Chassefiere, E., 1997. Loss of water on the young Venus: The effect of a strong primitive solar wind. Icarus 126, 229–232. doi:{10.1006/icar.1997.5677}.

- Coe, R.S., 1967. Determination of paleo-intensities of Earth's magnetic field with emphasis on mechanisms which could cause non-ideal behavior in Thelliers method. *Journal of Geomagnetism and Geoelectricity* 19, 157–179.
- Coe, R.S., Glatzmaier, G.A., 2006. Symmetry and stability of the geomagnetic field. *Geophysical Research Letters* 33. doi:{10.1029/2006GL027903}.
- Compston, W., Pidgeon, R.T., 1986. Jack Hills, evidence of more very old detrital zircons in Western-Australia. *Nature* 321, 766–769. doi:{10.1038/321766a0}.
- Cottrell, R.D., Tarduno, J.A., 1999. Geomagnetic paleointensity derived from single plagioclase crystals. *Earth and Planetary Science Letters* 169, 1–5. doi:{10.1016/S0012-821X(99)00068-0}.
- Cottrell, R.D., Tarduno, J.A., 2000. In search of high-fidelity geomagnetic paleointensities: A comparison of single plagioclase crystal and whole rock Thellier-Thellier analyses. *Journal of Geophysical Research-Solid Earth* 105, 23579–23594. doi:{10.1029/2000JB900219}.
- Cottrell, R.D., Tarduno, J.A., Davis, W.J., Mamajek, E., 2013. Constraining the geodynamo and magnetopause during earth's first billion years, in: *Eos, Trans. AGU, American Geophysical Union*. pp. V31E–07.
- Cottrell, R.D., Tarduno, J.A., Roberts, J., 2008. The Kiaman Reversed Polarity Superchron at Kiama: Toward a field strength estimate based on single silicate crystals. *Physics of the Earth and Planetary Interiors* 169, 49–58. doi:{10.1016/j.pepi.2008.07.041}.
- Cowley, S.W.H., Lewis, Z.V., 1990. Magnetic trapping of energetic particles on open dayside boundary layer flux tubes. *Planetary and Space Science* 38, 1343–1350. doi:10.1016/0032-0633(90)90137-F.
- Cranmer, S.R., Saar, S.H., 2011. Testing a Predictive Theoretical Model for the Mass Loss Rates of Cool Stars. *ApJ* 741, 54. doi:10.1088/0004-637X/741/1/54, arXiv:1108.4369.

- Dauphas, N., Kasting, J.F., 2011. Low $p(\text{CO}_2)$ in the pore water, not in the Archean air. *Nature* 474, E2–E3. doi:{10.1038/nature09960}.
- Dehant, V., Lammer, H., Kulikov, Y.N., Griessmeier, J.M., Breuer, D., Verhoeven, O., Karatekin, O., Van Hoolst, T., Korablev, O., Lognonne, P., 2007. Planetary magnetic dynamo effect on atmospheric protection of early Earth and Mars. *Space Science Reviews* 129, 279–300. doi:{10.1007/s11214-007-9163-9}. Workshop on Geology and Habitability of Terrestrial Planets, Int Space Sci Inst, Bern, SWITZERLAND, SEP 05-09, 2005.
- Denyszyn, S., Feinberg, J., Renne, P., Scott, G., 2013. Revisiting the age and paleomagnetism of the Modipe Gabbro of South Africa. *Precambrian Research* 328, 176–185.
- Dorren, J., Guinan, E., 1994. HD-129333 - The Sun in its infancy. *Astrophysical Journal* 428, 805–818. doi:{10.1086/174289}.
- Drake, J.J., Cohen, O., Yashiro, S., Gopalswamy, N., 2013. Implications of Mass and Energy Loss due to Coronal Mass Ejections on Magnetically Active Stars. *ApJ* 764, 170. doi:10.1088/0004-637X/764/2/170, arXiv:1302.1136.
- Dunlop, D., Buchan, K., 1977. Thermal remagnetization and paleointensity record of metamorphic rocks. *Physics of the Earth and Planetary Interiors* 13, 325–331. doi:{10.1016/0031-9201(77)90117-0}.
- Dunlop, D., "Ozdemir, O., 1997. *Rock Magnetism, Fundamentals and Frontiers*. Cambridge Univ. Press.
- Dunlop, D., Yu, Y., 2004. Intensity and polarity of the geomagnetic field during Precambrian time, in: *Timescales of the Paleomagnetic Field*, American Geophysical Union,. pp. 85–100.
- Dunlop, D., Zhang, B., "Ozdemir, O., 2005. Linear and nonlinear Thellier paleointensity behavior of natural minerals. *Journal of Geophysical Research-Solid Earth* 110, B01103. doi:{10.1029/2004JB003095}.

- Dwyer, C.A., Stevenson, D.J., Nimmo, F., 2011. A long-lived lunar dynamo driven by continuous mechanical stirring. *Nature* 479, 212–U84. doi:{10.1038/nature10564}.
- Edberg, N.J.T., Nilsson, H., Futaana, Y., Stenberg, G., Lester, M., Cowley, S.W.H., Luhmann, J.G., McEnulty, T.R., Opgenoorth, H.J., Fedorov, A., Barabash, S., Zhang, T.L., 2011. Atmospheric erosion of Venus during stormy space weather. *Journal of Geophysical Research-Space Physics* 116, A09308. doi:{10.1029/2011JA016749}.
- Edberg, N.J.T., Nilsson, H., Williams, A.O., Lester, M., Milan, S.E., Cowley, S.W.H., Franz, M., Barabash, S., Futaana, Y., 2010. Pumping out the atmosphere of Mars through solar wind pressure pulses. *Geophysical Research Letters* 37, L03107. doi:{10.1029/2009GL041814}.
- Elkins-Tanton, L.T., 2013. Planetary Science: Evolutionary dichotomy for rocky planets. *Nature* 497, 570–572.
- Evans, M.E., McElhinney, M.W., 1966. Paleomagnetism of Modipe Gabbro. *Journal of Geophysical Research* 71, 6053–6063.
- Feinberg, J., Scott, G., Renne, P., Wenk, H., 2005. Exsolved magnetite inclusions in silicates: Features determining their remanence behavior. *Geology* 33, 513–516. doi:{10.1130/G21290.1}.
- Feinberg, J.M., Denyszyn, S.W., Renne, P.R., Scott, G.R., 2010. The paleomagnetism and age of the Modipe Gabbro, South Africa. *Geochimica et Cosmochimica Acta* 74, A283. Conference on Goldschmidt 2010 - Earth, Energy, and the Environment, Knoxville, TN, JUN 13-18, 2010.
- Ferk, A., Leonhardt, R., Hess, K., Koch, S., Krasa, D., Egli, R., Winklhofer, M., Dingwell, D., 2012. Cooling rate dependence of the TRM of SD, PSD and MD particles, in: EGU General Assembly Conference Abstracts, pp. EGU2012–5244.

- Feulner, G., 2012. The faint young sun problem. *Reviews of Geophysics* 50, RG2006.
- Fuller, M., 1974. Lunar Magnetism. *Reviews of Geophysics* 12, 23–70. doi:{10.1029/RG012i001p00023}.
- Fuller, M., Cisowski, S.M., 1987. *Geomagnetism*. Academic Press. volume 2. chapter Lunar Magnetism. pp. 307–455.
- Garrick-Bethell, I., Weiss, B.P., Shuster, D.L., Buz, J., 2009. Early Lunar Magnetism. *Science* 323, 356–359. doi:{10.1126/science.1166804}.
- Gattacceca, J., Rochette, P., 2004. Toward a robust normalized magnetic paleointensity method applied to meteorites. *Earth and Planetary Science Letters* 227, 377–393. doi:{10.1016/j.epsl.2004.09.013}.
- Gill, J., Elmore, R., Engel, M., 2002. Chemical remagnetization and clay diagenesis: testing the hypothesis in the cretaceous sedimentary rocks of north-western montana. *Physics and Chemistry of the Earth* 27, 1121–1139.
- Goldblatt, C., Claire, M.W., Lenton, T.M., Matthews, A.J., Watson, A.J., Zahnle, K.J., 2009. Nitrogen-enhanced greenhouse warming on early Earth. *Nature Geoscience* 2, 891–896. doi:{10.1038/NGE0692}.
- Goldblatt, C., Zahnle, K.J., 2011. Faint young Sun paradox remains. *Nature* 474, E3–E4. doi:{10.1038/nature09961}.
- Goldstein, B.E., Neugebauer, M., Phillips, J.L., Bame, S., Gosling, J.T., McComas, D., Wang, Y.M., Sheeley, N.R., Suess, S.T., 1996. ULYSSES plasma parameters: latitudinal, radial, and temporal variations. *A&A* 316, 296–303.
- Gough, D.O., 1981. Solar interior structure and luminosity variations. *Solar Physics* 74, 21–34. doi:{10.1007/BF00151270}.
- Graham, J.W., 1949. The stability and significance of magnetism in sedimentary rocks. *Journal of Geophysical Research* 54, 131–167. doi:{10.1029/JZ054i002p00131}.

- Grießmeier, J., Stadelmann, A., Penz, T., Lammer, H., Selsis, F., Ribas, I., Guinan, E., Motschmann, U., Biernat, H., Weiss, W., 2004. The effect of tidal locking on the magnetospheric and atmospheric evolution of “Hot Jupiters”. *Astronomy & Astrophysics* 425, 753–762. doi:{10.1051/0004-6361:20035684}.
- Halls, H.C., 1991. The Matachewan dyke swarm, Canada - an early Proterozoic magnetic-field reversal. *Earth and Planetary Science Letters* 105, 279–292. doi:{10.1016/0012-821X(91)90137-7}.
- Hamano, K., Abe, Y., Genda, H., 2013. Emergence of two types of terrestrial planet on solidification of magma ocean. *Nature* 497, 607–610. doi:{10.1038/nature12163}.
- Haqq-Misra, J.D., Domagal-Goldman, S.D., Kasting, P., Kasting, J., 2008. A revised, hazy methane greenhouse for the Archean Earth. *Astrobiology* 8, 1127–1137.
- Hasenkopf, C.A., Freedman, M.A., Beaver, M.R., Toon, O.B., Tolbert, M.A., 2011. Potential climatic impact of organic haze on early Earth. *Astrobiology* 11, 135–149. doi:{10.1089/ast.2010.0541}.
- Hofmann, A., Wilson, A.H., 2007. Silicified basalts, bedded cherts and other sea floor alteration phenomena of the 3.4 Ga Nondweni greenstone belt, South Africa. *Developments in Precambrian Geology* 15, 571–605.
- Holzwarth, V., Jardine, M., 2007. Theoretical mass loss rates of cool main-sequence stars. *A&A* 463, 11–21. doi:10.1051/0004-6361:20066486, arXiv:astro-ph/0611430.
- Hunten, D.M., 1973. Escape of light gases from planetary atmospheres. *Journal of the Atmospheric Sciences* 30, 1481–1494. doi:{10.1175/1520-0469(1973)030<1481:TEOLGF>2.0.CO;2}.

- Hunten, D.M., Donahue, T.M., Walker, J.C.G., Kasting, J.F., 1989. Origin and evolution of planetary and satellite atmospheres. University of Arizona Press, Tucson, AZ. chapter Escape of atmospheres and loss of water. pp. 386–422.
- Irving, E., 1964. Paleomagnetism and Its Application to Geological and Geophysical Problems. John Wiley and Sons.
- Jackson, M.G., Jellinek, A.M., 2013. Major and trace element composition of the high He-3/He-4 mantle: Implications for the composition of a nonchondritic Earth. *Geochemistry Geophysics Geosystems* 14, 2954–2976. doi:{10.1002/ggge.20188}.
- Jakosky, B.M., Pepin, R.O., Johnson, R.E., Fox, J.L., 1994. Mars atmospheric loss and isotopic fractionation by solar-wind-induced sputtering and photochemical escape. *Icarus* 111, 271–288. doi:{10.1006/icar.1994.1145}.
- Jeans, J.H., 1925. The Dynamical Theory of Gases. Cambridge University Press, London.
- Johnson, R.E., 1990. Energetic Charged Particle Interactions with Atmosphere and Surfaces. Springer Verlag, New York.
- Judge, P.G., Solomon, S.C., Ayres, T.R., 2003. An estimate of the Sun’s ROSAT-PPSPC x-ray luminosities using SNOE-SXP measurements. *The Astrophysical Journal* 593, 534–548.
- Kars, M., Aubourg, C., Pozzi, J.P., Janots, D., 2012. Continuous production of nanosized magnetite through low grade burial. *Geochemistry, Geophysics, Geosystems* 13, Q08Z48.
- Kasting, J.F., 1988. Runaway and moist greenhouse atmospheres and the evolution of Earth and Venus. *Icarus* 74, 472–494. doi:{10.1016/0019-1035(88)90116-9}.
- Kasting, J.F., 2010. How to find a habitable planet. Princeton University Press, Princeton, N.J.

- Kiehl, J.T., Dickinson, R.E., 1987. A study of the radiative effects of enhanced atmospheric CO₂ and CH₄ on early Earth surface temperatures. *Journal of Geophysical Research-Atmospheres* 92, 2991–2998. doi:{10.1029/JD092iD03p02991}.
- Kistler, L.M., Galvin, A.B., Popecki, M.A., Simunac, K.D.C., Farrugia, C., Moebius, E., Lee, M.A., Blush, L.M., Bochsler, P., Wurz, P., Klecker, B., Wimmer-Schweingruber, R.F., Opitz, A., Sauvaud, J.A., Thompson, B., Russell, C.T., 2010. Escape of O⁺ through the distant tail plasma sheet. *Geophysical Research Letters* 37, L21101. doi:{10.1029/2010GL045075}.
- Kulikov, Y.N., Lammer, H., Lichtenegger, H.I.M., Penz, T., Breuer, D., Spohn, T., Lundin, R., Biernat, H.K., 2007. A comparative study of the influence of the active young Sun on the early atmospheres of Earth, Venus, and Mars. *Space Science Reviews* 129, 207–243. doi:{10.1007/s11214-007-9192-4}. Workshop on Geology and Habitability of Terrestrial Planets, Int Space Sci Inst, Bern, SWITZERLAND, SEP 05-09, 2005.
- Labrosse, S., Hernlund, J.W., Coltice, N., 2007. A crystallizing dense magma ocean at the base of the Earth’s mantle. *Nature* 450, 866–869. doi:{10.1038/nature06355}.
- Lammer, H., 2013. Origin and evolution of planetary atmosphere: Implications for habitability. Springer- Briefs in Astronomy, Springer Heidelberg.
- Lammer, H., Kasting, J.F., Chassefiere, E., Johnson, R.E., Kulikov, Y.N., Tian, F., 2008. Atmospheric escape and evolution of terrestrial planets and satellites. *Space Science Reviews* 139, 399–436. doi:{10.1007/s11214-008-9413-5}. Workshop on Comparative Aeronomy, ISSI, Bern, SWITZERLAND, JUN 25-29, 2007.
- Lawrence, K., Johnson, C., Tauxe, L., Gee, J., 2008. Lunar paleointensity measurements: Implications for lunar magnetic evolution. *Physics of the Earth and Planetary Interiors* 168, 71–87. doi:{10.1016/j.pepi.2008.05.007}.

- Lay, T., Hernlund, J., Buffett, B.A., 2008. Core-mantle boundary heat flow. *Nature Geoscience* 1, 25–32. doi:{10.1038/ngeo.2007.44}.
- Layer, P.W., Lopez-Martinez, M., Kroner, A., York, D., McWilliams, M., 1998. Thermochronometry and palaeomagnetism of the Archaean Nelshoogte Pluton, South Africa. *Geophysical Journal International* 135, 129–145. doi:{10.1046/j.1365-246X.1998.00613.x}.
- Le Bars, M., Wieczorek, M.A., Karatekin, O., Cebbron, D., Laneuville, M., 2011. An impact-driven dynamo for the early Moon. *Nature* 479, 215–U90. doi:{10.1038/nature10565}.
- Lichtenegger, H.I.M., Lammer, H., Griessmeier, J.M., Kulikov, Y.N., von Paris, P., Hausleitner, W., Krauss, S., Rauer, H., 2010. Aeronomical evidence for higher CO₂ levels during Earth’s Hadean epoch. *Icarus* 210, 1–7. doi:{10.1016/j.icarus.2010.06.042}.
- Lowe, D.R., Byerly, G.R., Kyte, F.T., Shukolyukov, A., Asaro, F., Krull, A., 2003. Spherule beds 3.47-3.24 billion years old in the Barberton Greenstone Belt, South Africa: A record of large meteorite impacts and their influence on early crustal and biological evolution. *Astrobiology* 3, 7–48. doi:{10.1089/153110703321632408}. 10th Rubey Colloquium, LOS ANGELES, CA, FEB 08-09, 2002.
- Luhmann, J.G., Johnson, R.E., Zhang, M.H.G., 1992. Evolutionary impact of sputtering of the Martian atmosphere by O⁺ pickup ions. *Geophysical Research Letters* 19, 2151–2154. doi:{10.1029/92GL02485}.
- Lundin, R., Lammer, H., Ribas, I., 2007. Planetary magnetic fields and solar forcing: Implications for atmospheric evolution. *Space Science Reviews* 129, 245–278. doi:{10.1007/s11214-007-9176-4}. Workshop on Geology and Habitability of Terrestrial Planets, Int Space Sci Inst, Bern, SWITZERLAND, SEP 05-09, 2005.

- Lyon, J.G., 2000. The solar wind-magnetosphere-ionosphere system. *Science* 288, 1987–1991. doi:{10.1126/science.288.5473.1987}.
- Mamajek, E.E., 2012. On the Age and Binarity of Fomalhaut. *ApJ Letters* 754, L20. doi:10.1088/2041-8205/754/2/L20, arXiv:1206.6353.
- Mamajek, E.E., Hillenbrand, L.A., 2008. Improved age estimation for solar-type dwarfs using activity-rotation diagnostics. *Astrophysical Journal* 687, 1264–1293. doi:{10.1086/591785}.
- Mamajek, E.E., Hillenbrand, L.A., 2008. Improved Age Estimation for Solar-Type Dwarfs Using Activity-Rotation Diagnostics. *ApJ* 687, 1264–1293. doi:10.1086/591785, arXiv:0807.1686.
- Marty, B., Zimmermann, L., Pujol, M., Burgess, R., Philippot, P., 2013. Nitrogen isotopic composition and density of the archean atmosphere. *Science* 342, 101–104. doi:10.1126/science.1240971.
- Moore, T.E., Khazanov, G.V., 2010. Mechanisms of ionospheric mass escape. *J. Geophys. Res.* 115, A00J13.
- Muxworthy, A.R., Evans, M.E., Scourfield, S.J., King, J.G., 2013. Paleointensity results from the late-Archaean Modipe Gabbro of Botswana. *Geochemistry Geophysics Geosystems* 14, 2198–2205. doi:{10.1002/ggge.20142}.
- Néel, L., 1949. Théorie du traînage magnétique des ferromagnétiques en grains fins avec applications aux terres cuites. *Ann. Geophys.* 5, 99–136.
- Néel, L., 1955. Some theoretical aspects of rock-magnetism. *Advances In Physics* 4, 191–243. doi:{10.1080/00018735500101204}.
- Nelson, J.M., Tarduno, J.A., Cottrell, R.D., Valley, J.W., 2010. Paleomagnetic investigation of sedimentary units from Jack Hills, Western Australia, containing Archean-Hadean minerals, in: *Eos, Trans. AGU, American Geophysical Union*. pp. GP33C–0952.

- Olson, P., 2013. The new core paradox. *Science* 342, 431–432. doi:{10.1126/science.1243477}.
- Opik, E.J., 1963. Selective escape of gases. *Geophysical Journal of the Royal Astronomical Society* 7, 490–509. doi:{10.1111/j.1365-246X.1963.tb07091.x}.
- Owen, T., Cess, R.D., Ramanathan, V., 1979. Enhanced CO₂ greenhouse to compensate for reduced solar luminosity on early Earth. *Nature* 277, 640–642. doi:{10.1038/277640a0}.
- Ozima, M., Seki, K., Terada, N., Miura, Y., Podosek, F., Shinagawa, H., 2005. Terrestrial nitrogen and noble gases in lunar soils. *Nature* 436, 655–659. doi:{10.1038/nature03929}.
- Ozima, M., Yin, Q.Z., Podosek, F.A., Miura, Y.N., 2008. Toward understanding early Earth evolution: Prescription for approach from terrestrial noble gas and light element records in lunar soils. *Proceedings of the National Academy of Sciences of the United States of America* 105, 17654–17658. doi:{10.1073/pnas.0806596105}.
- Parker, E.N., 1970. Origin of solar magnetic fields. *Annual Review of Astronomy and Astrophysics* 8, 1–30. doi:{10.1146/annurev.aa.08.090170.000245}.
- Paschmann, G., Oieroset, M., Phan, T., 2013. In-situ observations of reconnection in space. *Space Science Reviews* 178, 385–417. doi:{10.1007/s11214-012-9957-2}.
- de Pater, I., Lissauer, J.J., 2001. *Planetary Science*. Cambridge Univ. Press.
- Pecaut, M.J., Mamajek, E.E., 2013. Intrinsic Colors, Temperatures, and Bolometric Corrections of Pre-main-sequence Stars. *ApJS* 208, 9. doi:10.1088/0067-0049/208/1/9, arXiv:1307.2657.
- Peres, G., Orlando, S., Reale, F., Rosner, R., Hudson, H., 2000. The Sun as an X-Ray Star. II. Using the Yohkoh/Soft X-Ray Telescope-derived Solar Emis-

- sion Measure versus Temperature to Interpret Stellar X-Ray Observations. *ApJ* 528, 537–551. doi:10.1086/308136.
- Pierrehumbert, R., 2010. *Principles of Planetary Climate*. Cambridge Univ. Press, Cambridge, UK.
- Pullaiah, G., Irving, E., Buchan, K.L., Dunlop, D.J., 1975. Magnetization Changes Caused By Burial And Uplift. *Earth and Planetary Science Letters* 28, 133–143. doi:{10.1016/0012-821X(75)90221-6}.
- Rasmussen, B., Fletcher, I.R., Muhling, J.R., Wilde, S.A., 2010. In situ U-Th-Pb geochronology of monazite and xenotime from the Jack Hills belt: Implications for the age of deposition and metamorphism of Hadean zircons. *Precambrian Research* 180, 26–46. doi:{10.1016/j.precamres.2010.03.004}.
- Reinhard, C.T., Planavsky, N.J., 2011. Mineralogical constraints on Precambrian p(CO₂). *Nature* 474, E1–E2. doi:{10.1038/nature09959}.
- Ribas, I., Guinan, E.F., Gudel, M., Audard, M., 2005. Evolution of the solar activity over time and effects on planetary atmospheres. I. High-energy irradiances (1-1700 angstrom). *Astrophysical Journal* 622, 680–694. doi:{10.1086/427977}.
- Roberts, P.H., Glatzmaier, G.A., 2000. Geodynamo theory and simulations. *Reviews of Modern Physics* 72, 1081–1123. doi:{10.1103/RevModPhys.72.1081}.
- Rosenqvist, L., Opgenoorth, H., Buchert, S., McCrea, I., Amm, O., Lathuillere, C., 2005. Extreme solar-terrestrial events of October 2003: High-latitude and Cluster observations of the large geomagnetic disturbances on 30 October. *Journal of Geophysical Research-Space Physics* 110, A09S23. doi:{10.1029/2004JA010927}.
- Rosing, M.T., Bird, D.K., Sleep, N.H., Bjerrum, C.J., 2010. No climate paradox under the faint early Sun. *Nature* 464, 744–747. doi:{10.1038/nature08955}.

- Rosing, M.T., Bird, D.K., Sleep, N.H., Bjerrum, C.J., 2011. Rosing, Bird, Sleep & Bjerrum reply. *Nature* 474, E4–E5. doi:{10.1038/nature09962}.
- Sackmann, I.J., Boothroyd, A.I., 2003. Our Sun. V. A bright young Sun consistent with helioseismology and warm temperatures on ancient Earth and Mars. *Astrophysical Journal* 583, 1024–1039. doi:{10.1086/345408}.
- Sackmann, I.J., Boothroyd, A.I., 2003. Our Sun. V. A Bright Young Sun Consistent with Helioseismology and Warm Temperatures on Ancient Earth and Mars. *ApJ* 583, 1024–1039. doi:10.1086/345408, [arXiv:astro-ph/0210128](#).
- Sagan, C., Mullen, G., 1972. Earth and Mars - Evolution of atmospheres and surface temperatures. *Science* 177, 52–56. doi:{10.1126/science.177.4043.52}.
- Schrijver, C.J., Aschwanden, M.J., 2002. Constraining the properties of non-radiative heating of the coronae of cool stars and the Sun. *Astrophysical Journal* 566, 1147–1165. doi:{10.1086/324299}.
- Seager, S., 2010. *Exoplanet atmospheres- physical processes*. Princeton University Press, Princeton, N.J.
- Seki, K., Elphic, R.C., Hirahara, M., Terasawa, T., Mukai, T., 2001. On atmospheric loss of oxygen ions from Earth through magnetospheric processes. *Science* 291, 1939–1941. doi:{10.1126/science.1058913}.
- Selkin, P.A., Gee, J.S., Tauxe, L., Meurer, W.P., Newell, A.J., 2000. The effect of remanence anisotropy on paleointensity estimates: A case study from the Archean Stillwater Complex. *Earth and Planetary Science Letters* 183, 403–416. doi:{10.1016/S0012-821X(00)00292-2}.
- Shaw, G.H., 2008. Earth’s atmosphere - Hadean to early Proterozoic. *Chemie Der Erde-Geochemistry* 68, 235–264. doi:{10.1016/j.chemer.2008.05.001}.

- Shea, E.K., Weiss, B.P., Cassata, W.S., Shuster, D.L., Tikoo, S.M., Gattacceca, J., Grove, T.L., Fuller, M.D., 2012. A long-lived lunar core dynamo. *Science* 335, 453–456. doi:{10.1126/science.1215359}.
- Shue, J.H., Chao, J.K., Fu, H.C., Russell, C.T., Song, P., Khurana, K.K., Singer, H.J., 1997. A new functional form to study the solar wind control of the magnetopause size and shape. *J. Geophys. Res.* 102, 9497–9511.
- Siscoe, G.L., Chen, C.K., 1975. Paleomagnetosphere. *Journal of Geophysical Research-Space Physics* 80, 4675–4680. doi:{10.1029/JA080i034p04675}.
- Siscoe, G.L., Sibeck, D.G., 1980. Effects of non-dipole components on auroral-zone configurations during weak dipole field epochs. *Journal of Geophysical Research* 85, 3549–3556. doi:{10.1029/JB085iB07p03549}.
- Skumanich, A., 1972. Time Scales for CA II Emission Decay, Rotational Braking, and Lithium Depletion. *ApJ* 171, 565. doi:10.1086/151310.
- Smirnov, A.V., Tarduno, J.A., 2004. Secular variation of the Late Archean Early Proterozoic geodynamo. *Geophysical Research Letters* 31, L16607. doi:{10.1029/2004GL020333}.
- Smirnov, A.V., Tarduno, J.A., 2005. Thermochemical remanent magnetization in Precambrian rocks: Are we sure the geomagnetic field was weak? *Journal of Geophysical Research-Solid Earth* 110, B06103. doi:{10.1029/2004JB003445}.
- Smirnov, A.V., Tarduno, J.A., Evans, D.A.D., 2011. Evolving core conditions ca. 2 billion years ago detected by paleosecular variation. *Physics of the Earth and Planetary Interiors* 187, 225–231. doi:{10.1016/j.pepi.2011.05.003}.
- Smirnov, A.V., Tarduno, J.A., Pisakin, B.N., 2003. Paleointensity of the early geodynamo (2.45 Ga) as recorded in Karelia: A single-crystal approach. *Geology* 31, 415–418. doi:{10.1130/0091-7613(2003)031<0415:POTEGG>2.0.CO;2}.

- Spaggiari, C.V., 2007. The Jack Hills greenstone belt, Western Australia - Part 1: Structural and tectonic evolution over > 1.5 Ga. *Precambrian Research* 155, 204–228. doi:{10.1016/j.precamres.2007.02.007}.
- Spaggiari, C.V., Pidgeon, R.T., Wilde, S.A., 2007. The Jack Hills greenstone belt, Western Australia - Part 2: Lithological relationships and implications for the deposition of > 4.0 Ga detrital zircons. *Precambrian Research* 155, 261–286. doi:{10.1016/j.precamres.2007.02.004}.
- Stegman, D.R., Jellinek, A.M., Zatman, S.A., Baumgardner, J.R., Richards, M.A., 2003. An early lunar core dynamo driven by thermochemical mantle convection. *Nature* 421, 143–146. doi:{10.1038/nature01267}.
- Sterenborg, M.G., Cohen, O., Drake, J.J., Gombosi, T.I., 2011. Modeling the young Sun’s solar wind and its interaction with Earth’s paleomagnetosphere. *Journal of Geophysical Research-Space Physics* 116, A01217. doi:{10.1029/2010JA016036}.
- Stevenson, D.J., 1983. Planetary magnetic-fields. *Reports on Progress in Physics* 46, 555–620. doi:{10.1088/0034-4885/46/5/001}.
- Strangeway, R.J., Ergun, R.E., Su, Y.J., Carlson, C.W., Elphic, R.C., 2005. Factors controlling ionospheric outflows as observed at intermediate altitudes. *J. Geophys. Res.* 110, A03221.
- Strangeway, R.J., Russell, C.T., Luhmann, J.G., Moore, T.E., Foster, J.C., Barabash, S.V., Nilsson, H., 2010. Does a planetary-scale magnetic field enhance or inhibit ionospheric plasma outflows?, in: Fall Meeting, American Geophysical Union Meeting, American Geophysical Union. pp. SM33BB–1893.
- Strik, G., Blake, T.S., Zegers, T.E., White, S.H., Langereis, C.G., 2003. Palaeomagnetism of flood basalts in the Pilbara Craton, Western Australia: Late Archaean continental drift and the oldest known reversal of the geomag-

- netic field. *Journal of Geophysical Research-Solid Earth* 108, B12, 2551. doi:{10.1029/2003JB002475}.
- Suavet, C., Weiss, B.P., Cassata, W.S., Shuster, D.L., Gattacceca, J., Chan, L., Garrick-Bethell, I., Head, J.W., Grove, T.L., Fuller, M.D., 2013. Persistence and origin of the lunar core dynamo. *Proceedings of the National Academy of Sciences of the United States of America* 110, 8453–8458. doi:{10.1073/pnas.1300341110}.
- Suzuki, T.K., 2012. Solar wind and its evolution. *Earth Planets and Space* 64, 201–206. doi:{10.5047/eps.2011.04.012}.
- Suzuki, T.K., Imada, S., Kataoka, R., Kato, Y., Matsumoto, T., Miyahara, H., Tsuneta, S., 2013. Saturation of stellar winds from young stars. *Publ. Astron. Soc. Japan* 65, 98. doi:{10.1093/pasj/65.5.98}.
- Suzuki, T.K., Imada, S., Kataoka, R., Kato, Y., Matsumoto, T., Miyahara, H., Tsuneta, S., 2013. Saturation of Stellar Winds from Young Suns. *PASJ* 65, 98. doi:10.1093/pasj/65.5.98, [arXiv:1212.6713](#).
- Tarduno, J.A., 2009. Geodynamo history preserved in single silicate crystals: Origins and long-term mantle control. *Elements* 5, 217–222. doi:{10.2113/gselements.5.4.217}.
- Tarduno, J.A., Cottrell, R.D., 2005. Dipole strength and variation of the time-averaged reversing and nonreversing geodynamo based on Thellier analyses of single plagioclase crystals. *Journal of Geophysical Research-Solid Earth* 110, B11101. doi:{10.1029/2005JB003970}.
- Tarduno, J.A., Cottrell, R.D., 2013. Signals from the ancient geodynamo: A paleomagnetic field test on the Jack Hills metaconglomerate. *Earth and Planetary Science Letters* 367, 123–132. doi:{10.1016/j.epsl.2013.02.008}.
- Tarduno, J.A., Cottrell, R.D., Nimmo, F., Hopkins, J., Voronov, J., Erickson, A., Blackman, E., Scott, E.R.D., McKinley, R., 2012. Evidence for a dynamo

- in the main group pallasite parent body. *Science* 338, 939–942. doi:{10.1126/science.1223932}.
- Tarduno, J.A., Cottrell, R.D., Smirnov, A.V., 2001. High geomagnetic intensity during the mid-Cretaceous from Thellier analyses of single plagioclase crystals. *Science* 291, 1779–1783. doi:{10.1126/science.1057519}.
- Tarduno, J.A., Cottrell, R.D., Smirnov, A.V., 2002. The Cretaceous superchron geodynamo: Observations near the tangent cylinder. *Proceedings of The National Academy of Sciences of the United States of America* 99, 14020–14025. doi:{10.1073/pnas.222373499}.
- Tarduno, J.A., Cottrell, R.D., Smirnov, A.V., 2006. The paleomagnetism of single silicate crystals: Recording geomagnetic field strength during mixed polarity intervals, superchrons, and inner core growth. *Reviews of Geophysics* 44, RG1002. doi:{10.1029/2005RG000189}.
- Tarduno, J.A., Cottrell, R.D., Watkeys, M.K., Bauch, D., 2007. Geomagnetic field strength 3.2 billion years ago recorded by single silicate crystals. *Nature* 446, 657–660. doi:{10.1038/nature05667}.
- Tarduno, J.A., Cottrell, R.D., Watkeys, M.K., Hofmann, A., Doubrovine, P.V., Mamajek, E.E., Liu, D., Sibeck, D.G., Neukirch, L.P., Usui, Y., 2010. Geodynamo, solar wind, and magnetopause 3.4 to 3.45 billion years ago. *Science* 327, 1238–1240. doi:{10.1126/science.1183445}.
- Tarduno, J.A., Cottrell, R.D., Watkeys, M.K., Hofmann, A., Doubrovine, P.V., Mamajek, E.E., Liu, D., Sibeck, D.G., Neukirch, L.P., Usui, Y., 2010. Geodynamo, Solar Wind, and Magnetopause 3.4 to 3.45 Billion Years Ago. *Science* 327, 1238–. doi:10.1126/science.1183445.
- Telleschi, A., Güdel, M., Briggs, K., Audard, M., Ness, J.U., Skinner, S.L., 2005. Coronal Evolution of the Sun in Time: High-Resolution X-Ray Spectroscopy of Solar Analogs with Different Ages. *ApJ* 622, 653–679. doi:10.1086/428109, [arXiv:astro-ph/0503546](https://arxiv.org/abs/astro-ph/0503546).

- Thellier, E., Thellier, O., 1959. Sur l'intensité du champ magnetique terrestre dans le passé historique et géologique. *Ann. Geophys.* 15, 285–376.
- Tian, F., Kasting, J.F., Liu, H.L., Roble, R.G., 2008. Hydrodynamic planetary thermosphere model: 1. Response of the Earth's thermosphere to extreme solar EUV conditions and the significance of adiabatic cooling. *Journal of Geophysical Research-Planets* 113, E05008. doi:{10.1029/2007JE002946}.
- Tian, F., Toon, O.B., Pavlov, A.A., De Sterck, H., 2005. A hydrogen-rich early Earth atmosphere. *Science* 308, 1014–1017. doi:{10.1126/science.1106983}.
- Tice, M.M., Bostick, B.C., Lowe, D.R., 2004. Thermal history of the 3.5-3.2 Ga Onverwacht and Fig Tree Groups, Barberton greenstone belt, South Africa, inferred by Raman microspectroscopy of carbonaceous material. *Geology* 32, 37–40. doi:{10.1130/G19915.1}.
- Tilgner, A., 2005. Precession driven dynamos. *Physics of Fluids* 17, 034104. doi:{10.1063/1.1852576}.
- Toth, G., Sokolov, I., Gombosi, T., Chesney, D., Clauer, C., De Zeeuw, D., Hansen, K., Kane, K., Manchester, W., Oehmke, R., Powell, K., Ridley, A., Roussev, I., Stout, Q., Volberg, O., Wolf, R., Sazykin, S., Chan, A., Yu, B., Kota, J., 2005. Space Weather Modeling Framework: A new tool for the space science community. *Journal of Geophysical Research-Space Physics* 110, A12226. doi:{10.1029/2005JA011126}.
- Ushikubo, T., Kita, N.T., Cavosie, A.J., Wilde, S.A., Rudnick, R.L., Valley, J.W., 2008. Lithium in Jack Hills zircons: Evidence for extensive weathering of Earth's earliest crust. *Earth and Planetary Science Letters* 272, 666–676. doi:{10.1016/j.epsl.2008.05.032}.
- Usui, Y., Tarduno, J.A., Watkeys, M., Hofmann, A., Cottrell, R.D., 2009. Evidence for a 3.45-billion-year-old magnetic remanence: Hints of an ancient

- geodynamo from conglomerates of South Africa. *Geochemistry Geophysics Geosystems* 10, Q09Z07. doi:{10.1029/2009GC002496}.
- Valley, J.W., 2006. Early Earth. *Elements* 2, 201–204. doi:{10.2113/gselements.2.4.201}.
- Verwey, E.J.W., 1939. Electronic conduction of magnetite (Fe_3O_4) and its transition point at low temperatures. *Nature* 144, 327–328. doi:{10.1038/144327b0}.
- Vidotto, A.A., Opher, M., Jatenco-Pereira, V., Gombosi, T.I., 2009. Three-Dimensional Numerical Simulations of Magnetized Winds of Solar-Like Stars. *Astrophysical Journal* 699, 441–452. doi:{10.1088/0004-637X/699/1/441}.
- Wacey, D., Kilburn, M.R., Saunders, M., Cliff, J., Brasier, M.D., 2011. Microfossils of sulphur-metabolizing cells in 3.4-billion-year-old rocks of Western Australia. *Nature Geoscience* 4, 698–702. doi:{10.1038/NGEO1238}.
- Walker, J.D., Geissman, J.W., Bowring, S.A., Babcock, L.E., 2013. The Geological Society of America Geologic Time Scale. *Geological Society of America Bulletin* 125, 259–272. doi:10.1130/B30712.1.
- Walsh, B.M., Foster, J.C., Erickson, P.J., Sibeck, D.G., 2014. Simultaneous ground- and space-based observations of the plasmaspheric plume and reconnection. *Science* 343, 1122–1125. doi:10.1126/science.1247212.
- Watson, A.J., Donahue, T.M., Walker, J.C.G., 1981. The dynamics of a rapidly escaping atmosphere - applications to the evolution of Earth and Venus. *Icarus* 48, 150–166. doi:{10.1016/0019-1035(81)90101-9}.
- Watson, G.S., 1956. A test for randomness of directions. *Geophys. J. Int.* 7, 160–161.
- Weber, R.C., Lin, P.Y., Garnero, E.J., Williams, Q., Lognonne, P., 2011. Seismic detection of the lunar core. *Science* 331, 309–312. doi:{10.1126/science.1199375}.

- Wei, Y., Fraenz, M., Dubinin, E., Woch, J., Luehr, H., Wan, W., Zong, Q.G., Zhang, T.L., Pu, Z.Y., Fu, S.Y., Barabash, S., Lundin, R., Dandouras, I., 2012. Enhanced atmospheric oxygen outflow on Earth and Mars driven by a corotating interaction region. *Journal of Geophysical Research-Space Physics* 117, A03208. doi:{10.1029/2011JA017340}.
- Wilde, S.A., Valley, J.W., Peck, W.H., Graham, C.M., 2001. Evidence from detrital zircons for the existence of continental crust and oceans on the Earth 4.4 Gyr ago. *Nature* 409, 175–178. doi:{10.1038/35051550}.
- Williams, Q., Garnero, E.J., 1996. Seismic evidence for partial melt at the base of Earth’s mantle. *Science* 273, 1528–1530. doi:{10.1126/science.273.5281.1528}.
- Winklhofer, M., Fabian, K., Heider, F., 1997. Magnetic blocking temperatures of magnetite calculated with a three-dimensional micromagnetic model. *Journal of Geophysical Research-Solid Earth* 102, 22695–22709. doi:{10.1029/97JB01730}.
- Wood, B.E., 2006. The solar wind and the sun in the past. *Space Science Reviews* 126, 3–14. doi:{10.1007/s11214-006-9006-0}. Workshop on Solar Wind Interaction and Atmosphere Evolution of Mars, Kiruna, SWEDEN, FEB 27-MAR 01, 2006.
- Wood, B.E., Muller, H.R., Redfield, S., Edelman, E., 2014. Evidence for a weak wind from the young sun. *The Astrophysical Journal Letters* 781, L33.
- Wood, B.E., Müller, H.R., Redfield, S., Edelman, E., 2014. Evidence for a Weak Wind from the Young Sun. *ApJ Letters* 781, L33. doi:10.1088/2041-8205/781/2/L33.
- Wood, B.E., Muller, H.R., Zank, G.P., Linsky, J.L., Redfield, S., 2005. New mass-loss measurements from astrospheric Ly alpha absorption. *Astrophysical Journal* 628, L143–L146. doi:{10.1086/432716}.

- Wordsworth, R., Pierrehumbert, R., 2013. Hydrogen-Nitrogen greenhouse warming in Earth's early atmosphere. *Science* 339, 64–67. doi:{10.1126/science.1225759}.
- Wright, N.J., Drake, J.J., Mamajek, E.E., Henry, G.W., 2011. The Stellar-activity-Rotation Relationship and the Evolution of Stellar Dynamos. *ApJ* 743, 48. doi:10.1088/0004-637X/743/1/48, arXiv:1109.4634.
- Yoshihara, A., Hamano, Y., 2004. Paleomagnetic constraints on the Archean geomagnetic field intensity obtained from komatiites of the Barberton and Belingwe greenstone belts, South Africa and Zimbabwe. *Precambrian Research* 131, 111–142. doi:{10.1016/j.precamres.2004.01.003}.
- Yu, Y., 2011. Importance of cooling rate dependence of thermoremanence in paleointensity determination. *Journal of Geophysical Research-Solid Earth* 116, B09101. doi:{10.1029/2011JB008388}.
- Zhang, T.L., Delva, M., Baumjohann, W., Auster, H.U., Carr, C., Russell, C.T., Barabash, S., Balikhin, M., Kudela, K., Berghofer, G., Biernat, H.K., Lammer, H., Lichtenegger, H., Magnes, W., Nakamura, R., Schwingenschuh, K., Volwerk, M., Voros, Z., Zambelli, W., Fornacon, K.H., Glassmeier, K.H., Richter, I., Balogh, A., Schwarzl, H., Pope, S.A., Shi, J.K., Wang, C., Motschmann, U., Lebreton, J.P., 2007. Little or no solar wind enters Venus' atmosphere at solar minimum. *Nature* 450, 654–656. doi:{10.1038/nature06026}.

Supplementary Content

Reconstructing the Past Sun

We combine a theoretical stellar evolutionary track for a $1 M_{\odot}$ star with observational constraints on the time-evolution of various stellar parameters for Sun-like stars to produce a reconstruction of the Sun’s characteristics at geologically and astronomically relevant times (**Table 2**). The solar parameters are listed at the starts of various geological time periods, adopting recent ages from the Geological Society of America (Walker et al., 2013). We adopt the $1 M_{\odot}$ stellar evolutionary track from Bressan et al. (2012), which employs the recent Caffau et al. (2011) mixture for protosolar chemical composition. We make minor systematic shifts to the luminosity and effective temperature of the evolutionary track at the $\sim 1\%$ level in order to match the current Sun at an adopted meteoritic age for the solar system (4568 Myr; Bouvier and Wadhwa, 2010; Amelin et al., 2010). We adopt the revised stellar parameters compiled by Mamajek (2012): effective temperature $T_{\text{eff}} = 5772$ K, luminosity $L = 3.827 \times 10^{33} \text{ erg s}^{-1}$, and radius $R = 695660$ km. Spectral types were estimated through the new main sequence effective temperature scale of Pecaution and Mamajek (2013) (although in practice spectral types for G-stars are rarely quoted to better than ± 1 subtype precision). The X-ray luminosity evolution as a function of rotation was calibrated to the data from Wright et al. (2011), but was adjusted to pass through the Sun’s current combination of average X-ray luminosity and rotation period (parameterized via Rossby number; Mamajek and Hillenbrand, 2008). We have included an estimate of the mean emission-measure-averaged coronal temperature $\log \tilde{T}_X$ as a function of the Sun’s age, based on a custom fit to the data of Telleschi et al. (2005) and the modern Sun (Peres et al., 2000) as a function of mean X-ray luminosity in the ROSAT X-ray bandpass (L_X): $\log \tilde{T}_X \simeq -1.54 + 0.282 \log L_X$ (L_X in erg s^{-1}).

We estimate the Sun’s current average solar wind mass loss as follows. Based on $\sim 15,000$ daily solar wind measurements in the OmniWeb database¹ between 1963 and 2014, we estimate a mean daily solar wind density of $n = 6.94 \text{ cm}^{-3}$ and mean solar wind velocity of $V_{SW} = 439 \text{ km s}^{-1}$. Extrapolating these values over 4π steradians, one would estimate the solar wind mass loss rate to be $1.94 \times 10^{-14} \text{ M}_{\odot} \text{ yr}^{-1}$. Results from the Ulysses mission (Goldstein et al., 1996) show that at high heliographic latitude ($>20^{\circ}$) the solar wind has a product of density and velocity approximately half that at lower latitudes. We take this result into account and multiple our original estimate by $\sim 2/3$, leading to a spherically-averaged mean solar mass loss via solar wind of $\dot{M}_{\odot} = 1.3 \times 10^{-14} \text{ M}_{\odot} \text{ yr}^{-1}$.

Three mass loss rates are listed in Table 2: \dot{M}_W is estimated following the observational trends from Wood et al. (2014), \dot{M}_S is estimated following the simulations of Suzuki et al. (2013), and \dot{M}_{CME} is the estimated mass loss due solely to coronal mass ejections from flares (Drake et al., 2013). Magnetopause radii are estimated following Tarduno et al. (2010), assuming Earth magnetic field strengths equal to the current value ($R_{S,1}$) and half ($R_{S,1/2}$; similar to that measured for 3.45 Gya by Tarduno et al. 2010). Interplanetary magnetic field pressure was assumed to be negligible at all periods compared to the dynamical ram pressure of the wind.

Several of the stellar parameters for the Sun and Sun-like stars (mostly related to magnetic activity) are observationally well correlated with rotation period (e.g. Mamajek and Hillenbrand, 2008), so we made a careful reassessment of the Sun’s likely rotational evolution through study of Sun-like main sequence stars of different ages. Based upon a literature review of measured rotation rates of $\sim 1 \text{ M}_{\odot}$ ($\pm 10\%$) stars in ten young star clusters² and older field stars³ we derive a revised version of the Skumanich law (Skumanich, 1972): $P_{rot} =$

¹Goddard Space Flight Center Space Physics Data Facility:
<http://omniweb.gsfc.nasa.gov/>.

²In age order: Pleiades, M50, M35, M34, M11, Coma Ber, M37, Praesepe, Hyades, and NGC 6811.

³In age order: 18 Sco, Sun, α Cen A & B (mean), 16 Cyg B.

$25.5(t/t_{\odot})^{0.526 \pm 0.022}$ day, where t is stellar age, t_{\odot} is the Sun’s age (4568 Myr), and the relation is empirically constrained between ~ 0.1 -7 Gyr. A fit of Sun-like stars in young clusters and (older) field stars *omitting* the Sun, yields a nearly identical relation, *predicting* the modern Sun’s rotation period to be 25.4 day. We surmise that the Sun is a normal rotator (within ± 1 day) for its mass and age.

Has mass loss via the solar wind had an impact on the Sun’s luminosity evolution since reaching the main sequence? An enhanced early solar wind has been proposed to be a potential solution to the Faint Young Sun paradox (e.g. Sackmann and Boothroyd, 2003). We have surveyed the recent literature for published mass loss estimates and trends for Sun-like stars, as a function of age and/or X-ray luminosity, as well as theoretical predictions (e.g. Holzwarth and Jardine, 2007; Cranmer and Saar, 2011; Drake et al., 2013; Suzuki et al., 2013; Wood et al., 2014). Thus far, these recent studies are consistent with a total solar main sequence mass loss in the range ~ 0.01 -0.4%. In the same period, the Sun has lost $\sim 0.03\%$ of its mass due to radiative losses through converting mass to energy (Sackmann and Boothroyd, 2003). The Bressan et al. (2012) stellar evolutionary tracks are consistent with having zero-age main sequence luminosities of $L_{ZAMS} \simeq 0.70 (M/M_{\odot})^{4.535} L_{\odot}$ for solar composition stars within 10% of a solar mass. After 4.6 Gyr, the total predicted solar mass loss due to solar wind and radiative losses is in the range ~ 0.04 -0.4%, so the Sun could have plausibly been negligibly more luminous (~ 0.2 -1.8%) early in its main sequence phase. Hence, current observational and theoretical constraints on the mass loss history of the Sun seem inconsistent with enhanced early stellar winds providing a parsimonious solution to the Faint Young Sun paradox (e.g. Sackmann and Boothroyd, 2003).

Table 2: Solar Parameters: Zero-Age Main Sequence to Present

τ Gya	Age Gyr	T_{eff} K	Spec. Type	Lum. L/L_{\odot}	Rad. R/R_{\odot}	$\log R_X$ dex	$\log L_X$ ergs s^{-1}	$\log \tilde{T}_X$ K	\dot{M}_W $M_{\odot} \text{ yr}^{-1}$	\dot{M}_S $M_{\odot} \text{ yr}^{-1}$	\dot{M}_{CME} $M_{\odot} \text{ yr}^{-1}$	$R_{S,1}$ R_{Earth}	$R_{S,1/2}$ R_{Earth}	Name of Starting Geological Period ...
4.525	0.045	5630	G5.4V	0.686	0.871	-3.33	30.1	6.96	-12.6	-11.5	-10.1	4.7	3.7	<i>Zero-Age Main Sequence (ZAMS)</i>
4.450	0.120	5645	G5.2V	0.707	0.879	-3.92	29.5	6.79	-13.4	-11.9	-10.9	5.5	4.4	<i>Pleiades Cluster Age</i>
4.000	0.570	5660	G5.0V	0.735	0.891	-4.85	28.6	6.54	-12.0	-12.7	-12.3	7.0	5.6	Archaean Eon/Eoarchean Era
3.920	0.650	5662	G4.9V	0.739	0.893	-4.93	28.5	6.51	-12.1	-12.8	-12.4	7.2	5.7	<i>Hyaenes Cluster Age</i>
3.600	0.970	5672	G4.4V	0.756	0.900	-5.18	28.3	6.45	-12.4	-13.0	-12.7	7.7	6.1	Paleoarchean Era
3.450	1.120	5676	G4.2V	0.764	0.904	-5.27	28.2	6.42	-12.5	-13.0	-12.9	7.8	6.2	Barberton Greenstone Belt dacite
3.200	1.370	5684	G3.9V	0.777	0.909	-5.40	28.1	6.39	-12.7	-13.1	-13.1	8.1	6.4	Mesoarchean Era
2.800	1.770	5696	G3.6V	0.800	0.918	-5.56	27.9	6.35	-12.9	-13.2	-13.4	8.4	6.7	Neoarchean Era
2.500	2.070	5705	G3.4V	0.818	0.926	-5.67	27.8	6.32	-13.0	-13.3	-13.6	8.6	6.8	Proterozoic Eon
2.300	2.270	5710	G3.2V	0.830	0.931	-5.73	27.8	6.30	-13.1	-13.4	-13.7	8.8	6.9	Rhyacian Period
2.050	2.520	5718	G3.1V	0.846	0.937	-5.81	27.7	6.28	-13.2	-13.4	-13.8	8.9	7.1	Orosirian Period
1.800	2.770	5725	G2.9V	0.862	0.944	-5.87	27.6	6.27	-13.3	-13.5	-13.9	9.0	7.2	Strathairian Period
1.600	2.970	5731	G2.8V	0.876	0.949	-5.92	27.6	6.25	-13.3	-13.5	-14.0	9.1	7.2	Mesoproterozoic Era
1.400	3.170	5736	G2.7V	0.890	0.955	-5.97	27.6	6.24	-13.4	-13.5	-14.1	9.2	7.3	Ectasian Period
1.200	3.370	5742	G2.6V	0.904	0.961	-6.01	27.5	6.23	-13.4	-13.6	-14.2	9.3	7.4	Stenian Period
1.000	3.570	5747	G2.5V	0.919	0.967	-6.06	27.5	6.22	-13.5	-13.6	-14.2	9.4	7.5	Tonian Period
0.850	3.720	5751	G2.4V	0.930	0.971	-6.08	27.5	6.22	-13.5	-13.6	-14.3	9.4	7.5	Cryogenian Period
0.635	3.935	5757	G2.3V	0.947	0.978	-6.13	27.4	6.21	-13.6	-13.6	-14.4	9.5	7.6	Ediacaran Period
0.541	4.029	5759	G2.2V	0.954	0.981	-6.15	27.4	6.20	-13.6	-13.6	-14.4	9.6	7.6	Cambrian Period
0.485	4.085	5760	G2.2V	0.959	0.983	-6.15	27.4	6.20	-13.6	-13.7	-14.4	9.6	7.6	Ordovician Period
0.444	4.126	5762	G2.2V	0.962	0.985	-6.17	27.4	6.20	-13.6	-13.7	-14.4	9.6	7.6	Silurian Period
0.419	4.151	5762	G2.2V	0.964	0.985	-6.17	27.4	6.20	-13.6	-13.7	-14.4	9.6	7.6	Devonian Period
0.359	4.211	5764	G2.2V	0.969	0.987	-6.18	27.4	6.20	-13.6	-13.7	-14.5	9.6	7.6	Carboniferous Period
0.299	4.271	5765	G2.1V	0.974	0.990	-6.19	27.4	6.19	-13.7	-13.7	-14.5	9.7	7.7	Permian Period
0.252	4.318	5766	G2.1V	0.978	0.991	-6.20	27.4	6.19	-13.7	-13.7	-14.5	9.7	7.7	Triassic Period
0.201	4.369	5767	G2.1V	0.983	0.993	-6.21	27.4	6.19	-13.7	-13.7	-14.5	9.7	7.7	Jurassic Period
0.145	4.425	5769	G2.1V	0.988	0.995	-6.22	27.4	6.19	-13.7	-13.7	-14.5	9.7	7.7	Cretaceous Period
0.066	4.504	5771	G2.0V	0.994	0.998	-6.23	27.3	6.18	-13.7	-13.7	-14.5	9.7	7.7	Paleogene Period
0.023	4.547	5771	G2.0V	0.998	0.999	-6.24	27.3	6.18	-13.7	-13.7	-14.6	9.7	7.7	Neogene Period
0.003	4.567	5772	G2.0V	1.000	1.000	-6.24	27.3	6.18	-13.7	-13.7	-14.6	9.7	7.7	Quaternary Period

Figures

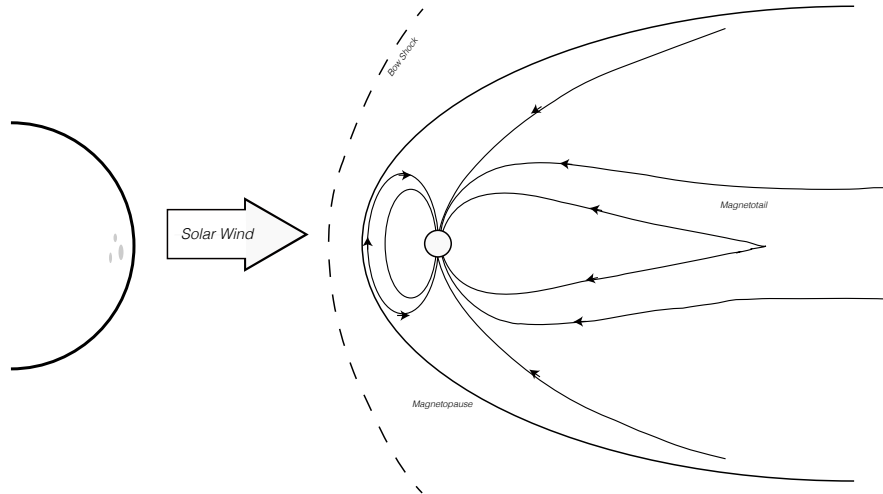


Figure 1

Figure 1: Magnetosphere (not to scale) shaped by the interaction of the solar wind (with pressure P_{sw} and Earth magnetic field (M_E)). The point where the solar wind pressure is balanced by the magnetic field is the standoff distance (r_s).

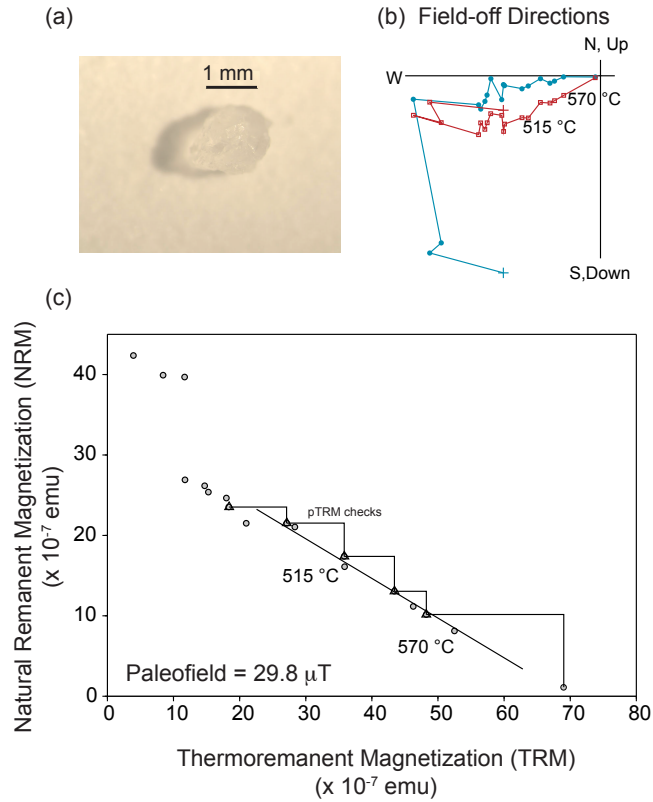


Figure 2

Figure 2: Example Thellier-Coe paleointensity experiment conducted on a single silicate crystal. a. Sample analyzed (quartz phenocryst with magnetite inclusions). b. Orthogonal vector plot of “field off” steps (see text). These define a component that trends toward the origin between approximately 515 and 570 °C. Red is inclination, blue is declination (note absolute orientation is arbitrary because the sample is unoriented). (c) Natural remanent magnetization (NRM) lost versus thermoremanent magnetization gained (TRM). TRM was acquired using an applied field of 60 μT . The slope of the line, for the temperature range where field-off data show linear decay to the origin (b) defines the paleofield strength. Example from (Tarduno et al., 2010).

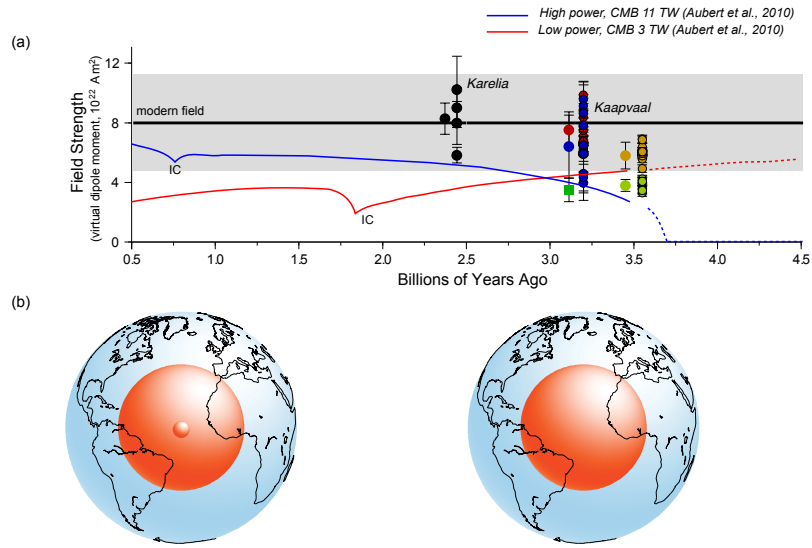


Figure 3

Figure 3: Archean paleointensity constraints based on single silicate crystal paleointensity and inner core growth. a. Field strength values are from Karelia (black, (Smirnov et al., 2003) at ~ 2.5 Ga, the Kaapvaal Craton at 3.2 Ga (red, blue, circles (Tarduno et al., 2007) and 3.4-3.45 Ga (yellow, green, circles (Tarduno et al., 2010)). Individual determinations (outlined circles) for the Kaapvaal craton are shown with mean (to left, circles without outlines). Green square is the 3.2 Ga data corrected for cooling rate. As discussed in the text, this cooling rate correction probably results in an underestimate of the true field value. Also shown are two models for field intensity history from (Aubert et al., 2010) based on high/low values of present-day core-mantle boundary heat flow. IC is the time of onset of inner core growth for the models. Many recent models invoke the onset of inner core growth younger than 1 Ga (b). In nearly all models, a long-lived Paleoproterozoic geodynamo would need to be entirely thermally driven.

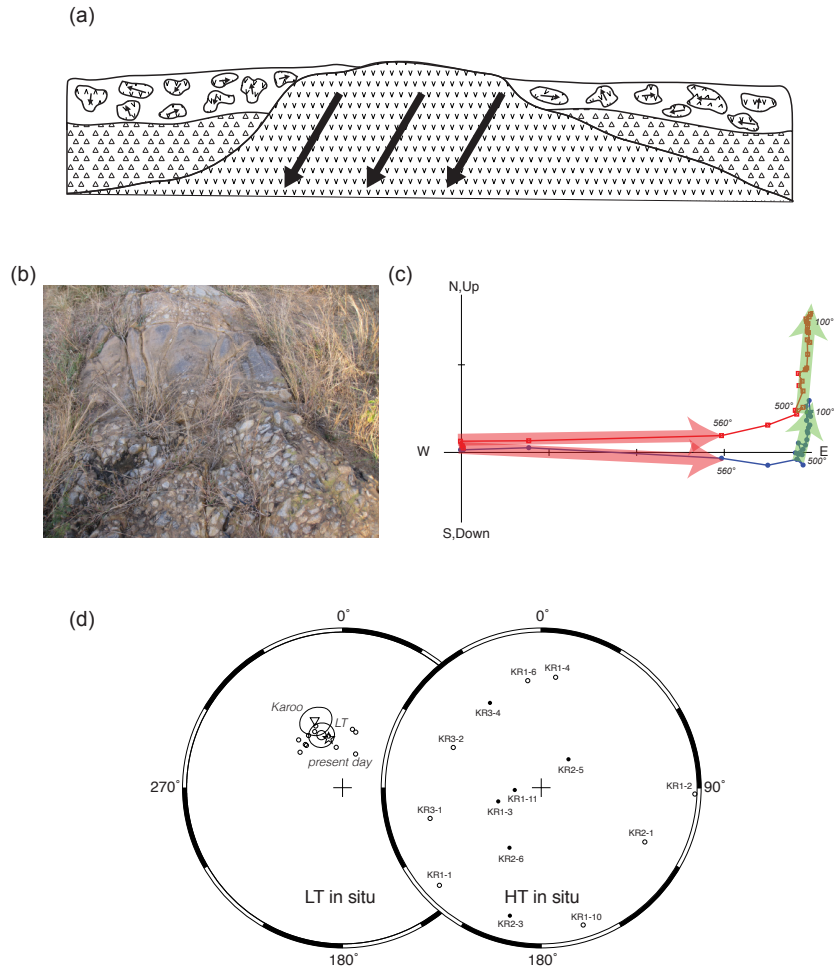


Figure 4

Figure 4: Conglomerate test on ~3.4 Ga rock unit from the Barberton Greenstone Belt (Kaapvaal Craton). a. Sketch of conglomerate formation. Key: “v” symbol, dacite; triangles, chert; arrows, imparted thermoremanent magnetization. b. Field photo of 3.4 Ga conglomerate. c. Orthogonal vector plot of stepwise thermal demagnetization of dacite clast from conglomerate; red is inclination, blue is declination. (b). Two components are defined at low unblocking temperatures (LT, green) and high unblocking temperatures (HT, red). d. Stereonet plots show that the LT component is well-grouped, as expected for a secondary magnetization. The HT component is scattered, as expected for a primary magnetization (cf. part a). (c) and (d) are from Usui et al. (Usui et al., 2009).

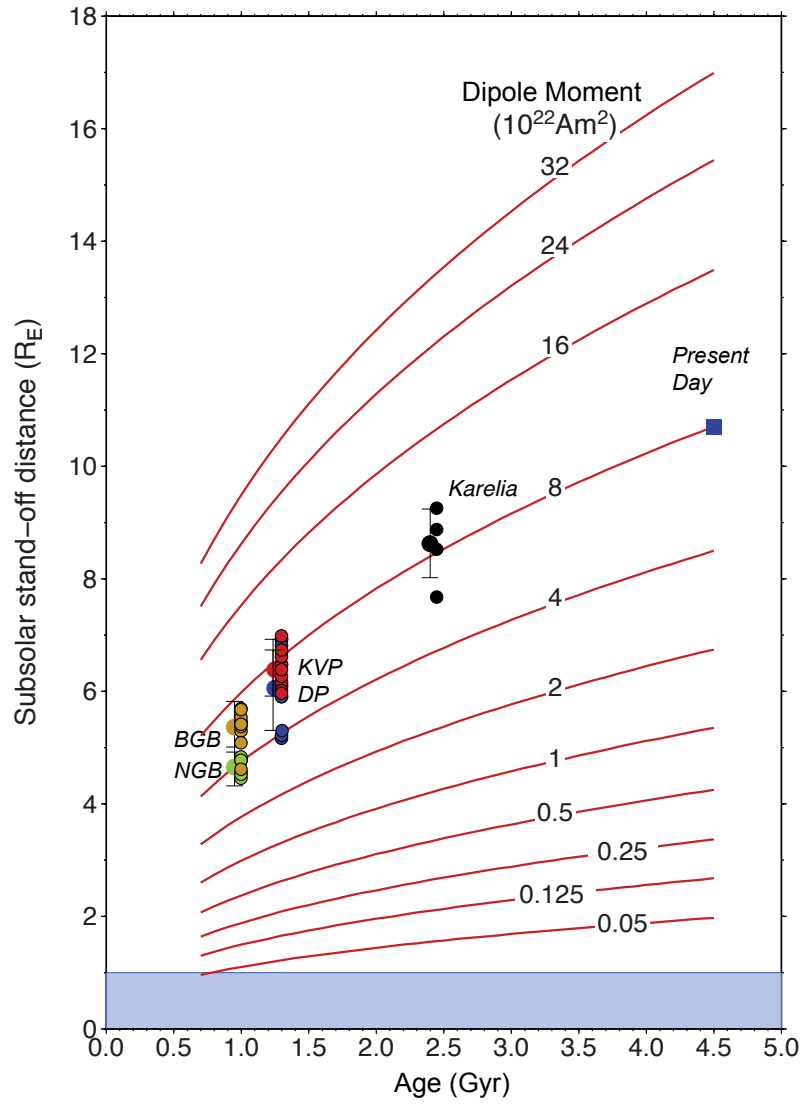


Figure 5

Figure 5: Standoff versus time. Subsolar standoff distance in Earth radii (R_E) plotted versus age from solar mass loss Model A (see text). Contours are Earth's dipole moment, with paleointensity data from single silicate crystals (cf. Figure 3). Figure modified from (Tarduno et al., 2010).

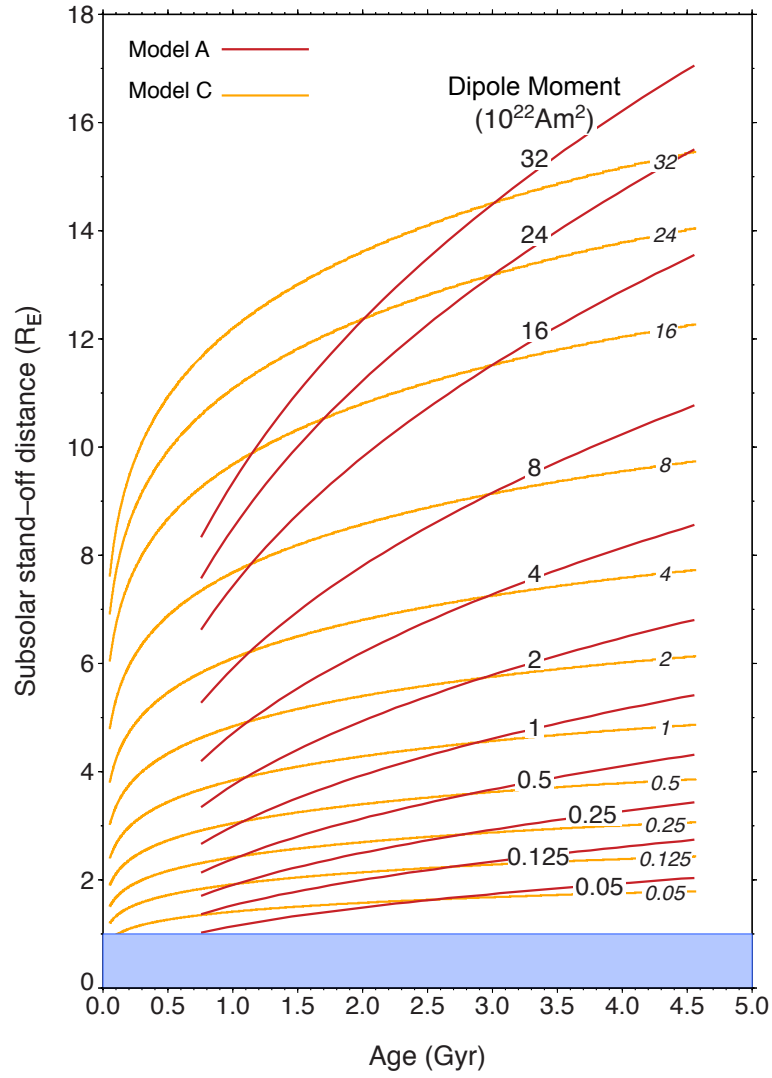


Figure 7

Figure 7: Standoff for solar ages younger than 700 Myr. Subsolar standoff distance in Earth radii (R_E) plotted versus age from solar mass loss Model A (red contours) versus Model C (yellow contours; see text).

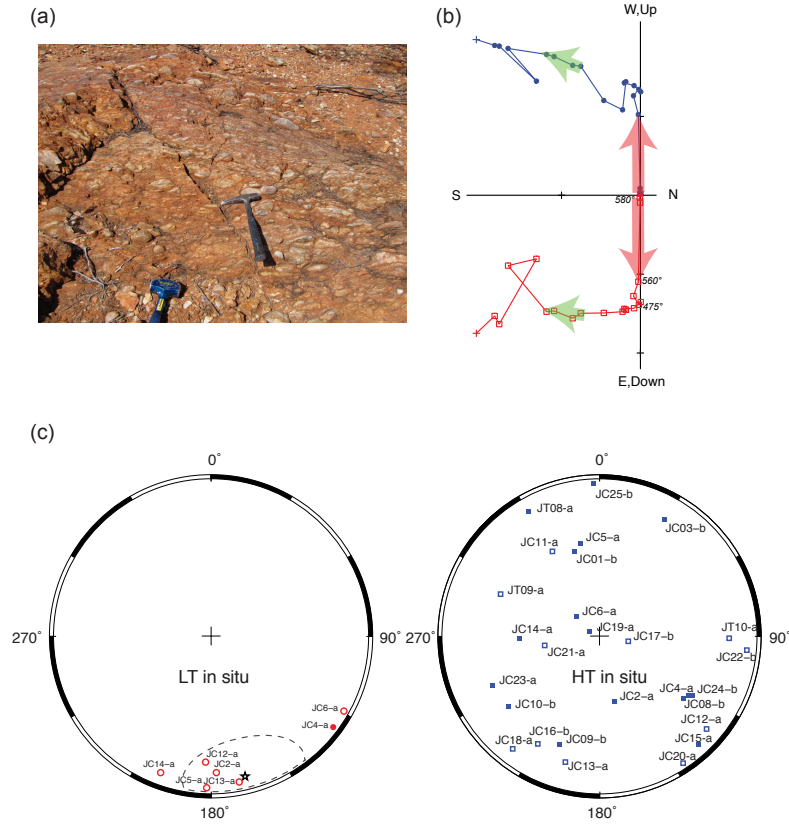


Figure 8

Figure 8: Conglomerate test on ~3.0 Ga metasediments from the Jack Hills (Yilgarn Craton). a. Field photo of conglomerate with cobble-sized clasts. b. Orthogonal vector plot of stepwise thermal demagnetization of subsample from interior of clast from conglomerate; red is inclination, blue is declination. Two components are defined at relatively low-intermediate unblocking temperatures (LT, green arrows) and high unblocking temperatures (HT, red arrows). Example from (Tarduno and Cottrell, 2013). Note that the E-W labels on the diagram were inadvertently inverted in the original publication. c. Stereonet plots show that a relatively well-grouped LT component from some clasts (left), as expected for a secondary magnetization. The HT component is scattered (right), as expected for a primary magnetization (from (Usui et al., 2009)).